

Report UCBTH08-003

Risk-informed Design Guidance for Advanced Reactor Concepts:
A Case Study of the Pebble Bed Advanced High Temperature Reactor

by

Edward David Blandford

B.S., Mechanical Engineering (University of California, Los Angeles) 2002

A project submitted in partial satisfaction of the

requirements for the degree of

Master of Science

In

Nuclear Engineering

in the

Graduate Division

of the

University of California, Berkeley

Committee in charge:
Professor William Kastenberg, Chair
Professor Per Peterson
Professor Ivan Catton (UCLA)

Spring 2008

Abstract

Efforts led principally by the DOE have identified several viable advanced nuclear reactor concepts each with their own respective advantages. The first advanced reactor paper concept to see commercial success will have demonstrated at a minimum the following three inter-related attributes: (1) licensing feasibility, (2) reduction in construction time, and (3) investment risk commensurate with alternative base-load generation options. Fundamental design changes such as single-phase working fluids, high temperature refractory materials, and passive safety features greatly reduce the complexity in assessing the risk associated with advanced reactors but also present a new set of licensing concerns. The modular Pebble Bed Advanced High Temperature Reactor (PB-AHTR) with a nominal power output of 900 MWth is the most recent version of the liquid fluoride salt Gen IV reactor types. Due to the high volumetric capacity of the primary coolant, the PB-AHTR operates with a high power density core achieving the same outlet temperature as competitive high temperature gas reactors. The reactivity control system for the PB-AHTR consists of a novel buoyantly-driven shutdown rod system that is passively activated during reactor transients. In addition to a traditional rod-type control rod system, the new shutdown rod system is designed to operate both actively and passively fulfilling both the role of a second reactivity control system and poison addition. Due to the relatively high density of the flibe, ${}^7\text{Li}_2\text{BeF}_4$, the shutdown rods consists of a graphite and B_4C blend mixture in a geometry maximizing worth while minimizing the parasitic drag force acting on the rod. The physical response of the shutdown rod was simulated both computationally and experimentally using scaling arguments where applicable with an emphasis on key phenomena identified during a PIRT study. Results from a preliminary risk-based reliability assessment indicate the PB-AHTR shutdown rod system is capable of achieving comparable levels of reliability as equivalent active reactivity control systems.

Table of Contents

Abstract	2
1 Introduction	5
1.1 History of Domestic Commercial Reactor Development and Licensing	5
1.1.1 Governing Code of Federal Regulations	6
1.2 Transition to Licensing Generation IV Reactors	7
1.2.1 Licensing of the PBMR	8
2 Case Study: Modular PB-AHTR Reactivity Control	18
2.1 PB-AHTR Overview	18
2.1.1 Key Safety Features	20
2.1.2 State of Technology	21
2.3 Description of PB-AHTR Reactivity Control System (RCS)	22
2.3.1 Reactivity Control and Protection System Functionality and Modes of Operation	24
2.3.1 Buoyant Shutdown Rod Concept	26
3 Phenomena Identification and Ranking	31
3.1 PIRT Generation Procedure	31
3.1.1 Application of PIRT to Shutdown Rod System Response	32
3.1.2 Selection of Nucleus Set of Event and Primary Safety Criteria	33
3.1.3 Identification of Associated Components	34
3.1.4 Identification of Major Processes and Phenomena	36
3.1.5 Ranking by PIRT Panel	Error! Bookmark not defined.
3.1.6 Evaluation of Knowledge Level Ranks	42
4 Passive Rod Insertion Shutdown Model (PRISM) Experiment	43
4.1 Sizing of the PRISM Experiment	43
4.1.1 Geometric similarity	43
4.1.2 Kinematic similarity	44
4.1.3 Dynamic similarity	44
4.2 PRISM Description	45
4.3 Experimental Results	50

4.3.1	Initial Calibration	50
4.3.2	PRISM Transient Simulations	52
4.4	Future PRISM Work	55
5	Methods for Assessing Passive Safety System Reliability – Case Study: SRS	57
5.1	Failure Modes for the Safety Shutdown Rod System	58
5.1.1	Structural Failure Modes.....	60
5.1.2	Hardware Failure Modes.....	62
5.1.3	Functional Failure Modes	63
5.1.4	FMEA Approach.....	Error! Bookmark not defined.
5.2	Probability of Failure for the SRS.....	Error! Bookmark not defined.
5.3	Treatment of Uncertainties in Passive Systems	64
6	Conclusion	66
7	References	67
	Appendix A – Safety Rod Performance Model	70
A.1	Dynamic Response of the PB-AHTR Safety Rod.....	70
A.2	Model Assumptions	70
A.3	PB-AHTR Safety Rod Dynamic Response under Transient Conditions	72
A.3.1	Momentum Balance on the Shutdown Rod System	72
A.3.2	Energy Balance on Channel Control Volume.....	74
A.3.3	Mass Conservation in Mixing Volume	74
	Appendix B – Effects of Buoyant Jet in PRISM	75
	Appendix C – Experimental Results from PRISM Phase I	76

1 Introduction

Advanced reactor technology, defined as Generation III+ and Generation IV concepts and beyond, has made great strides over the last 10 years due primarily to a recovery in the nuclear industry and consequent ripple effects in the research community. The number of utilities announcing their intent to construct new plants is increasing as favorable lending program (recently passed in the 2005 Energy Bill) and tried-LWR technology advancements have driven down financial risks. In addition to the Gen III+ reactors (i.e. ESBWR, AP-1000, EPR, etc...) being constructed, there has been a renewal in interest chiefly in high temperature gas reactor (HTGR) technology. The DOE identified the Very High Temperature Reactor (VHTR) as its highest priority of the six designs considered in the 2002 Generation IV Roadmap (Gen IV, 2002). The VHTR has been the focus of the Next Generation Nuclear Plant (NGNP) project, while the Global Nuclear Energy Partnership (GNEP) has focused on the sodium fast reactor (SFR).

Internationally, the Pebble Bed Modular Reactor (PBMR) group is preparing to build a commercial scale demonstration HTGR at Koeberg near Cape Town, where Africa's only nuclear power station is located, and a fuel plant at Pelindaba near Pretoria, where the pebble fuel will be manufactured. Assuming the required regulatory approvals are obtained, the current schedule will start construction of the demonstration plant in 2010 and load the first fuel in 2011. Construction of the first commercial modules are planned to start three years after successful demonstration of the first reactor. Additionally, HTGR test facilities have been or are scheduled to be built in Japan and Korea with an emphasis on hydrogen production.

1.1 History of Domestic Commercial Reactor Development and Licensing

Prior to the inception of the Nuclear Regulatory Commission (NRC) in 1975, nuclear technology was regulated by the Atomic Energy Commission (AEC). The AEC was first established by Congress in the Atomic Energy Act of 1946 and was subsequently authorized in 1954 to promote and regulate the commercialization of nuclear power plants. Due to the intrinsic conflict between promotion and regulation, Congress abolished the AEC and set up the Nuclear Regulatory Commission (NRC) with to the responsibility to regulate civilian nuclear activities to protect public health and safety. One of the key historical focuses of the AEC and NRC was their responsibility to develop regulatory requirements to protect the public from potential releases of radiation from a commercial nuclear power plants.

The focus of the regulatory programs of the AEC and the NRC was the prevention of major reactor accidents that would threaten public health and safety. Both agencies issued a series of requirements designed to make certain that a massive release of radiation from a power reactor

would be highly unlikely. During the late 1960s and 1970s, the nuclear industry was expanding rapidly with utilities placing large orders (a one year record of 43 orders were placed in 1973 by U.S. utilities). Along with an influx of LWR applications, scrutiny of key reactor safety issues such as safety equipment reliability, institutional regulations, and nuclear waste became much more prevalent in public discussion. In addition to LWR applications, a small gas reactor program was started and the NRC issued operating licenses for two high-temperature gas reactor (HTGR) plants at Peach Bottom 1 and Ft. St. Vrain. These licenses were based on a combination of interpretations of and exceptions to the LWR-based requirements and were not based on risk-informed and performance-based regulation policies (Silady, 2005). While Ft. St. Vrain became a major investment liability, the reasons for ultimately shutting down operation were unpredictable performance and excessive down time, rather than safety issues.

As of the February 27th 2008, the NRC expects to receive 22 new nuclear power plant license applications for 33 new units during the period from 2007 to 2010. These applications are for Gen III+ designs such as the Westinghouse AP-1000, General Electric ESBWR, and Areva EPR designs (NRC homepage). The main motivation behind Gen III+ systems is to present an economically competitive licensed reactor design based largely upon existing LWR technology that minimizing financial risk to the customer (i.e. utility, chemical manufacturer, etc.).

1.1.1 Governing Code of Federal Regulations

All federal regulations pertaining to energy generation fall under Title 10 where the first 199 parts are dedicated to the NRC. Of these parts, three of them make up a majority of the regulatory framework for licensing nuclear power plants:

- 10 CFR Part 50 - DOMESTIC LICENSING OF PRODUCTION AND UTILIZATION FACILITIES
- 10CFR Part 52 - EARLY SITE PERMITS; STANDARD DESIGN CERTIFICATIONS; AND COMBINED LICENSES FOR NUCLEAR POWER PLANTS
- 10CFR Part 100 - REACTOR SITE CRITERIA

The remaining parts of the NRC section cover a wide range of issues from the medical use of byproduct material to the documentation of public records. The three parts listed above will be referenced repeatedly throughout this work and can be located in the NRC reading room in their entirety. This regulatory structure has evolved substantially over several decades, mostly without the insights from probabilistic risk assessments (PRAs) and severe accident research. Much of the NRC's current activity focuses on regulation in 10 CFR Part 52 as utilities are applying for early site permits (ESP) and combined construction and operation licenses (COL). While issues such as spent fuel management and nuclear security are also important to the NRC, the work reported here focuses primarily on the reactor design process and does not address these other topics directly.

1.2 Transition to Licensing Generation IV Reactors

With the current NRC focus being on Gen III+ licensees and issues surrounding the currently operating fleet of LWR's, the NRC's recent effort to develop a technology-neutral licensing approach (NRC, 2004) for Gen IV reactor types has become a lower priority effort. The two recent exceptions to this has been serious advancements in the South African PBMR technology program which has revitalized the Exelon PBMR licensing effort originally initiated in 2001 and the maturation of the Next Generation Nuclear Project (NGNP) which calls for the use of a VHTR to generate hydrogen. Much of the currently existing regulatory guidelines are too LWR-specific and need to be changed to account for the significant advancements made in areas such as reactor materials and safety. In practice, the NRC will not issue revised licensing regulations until a group (that includes at least one major NSSS vendor) has made a significant financial investment to the licensing process.

The latest in NRC efforts on advanced reactor licensing can be found in a technology neutral licensing framework (NRC, 2005) developed by the Staff in addition to submittals and requests for additional information (RAI) between the PBMR group and the Staff. It is the intention of the Staff to ultimately to codify a technology-neutral regulatory structure for new plant licensing in a new stand-alone part in 10 CFR (NRC, 2004). The overall flow process the NRC is using to develop technology-neutral regulations is illustrated in Figure 0-1.

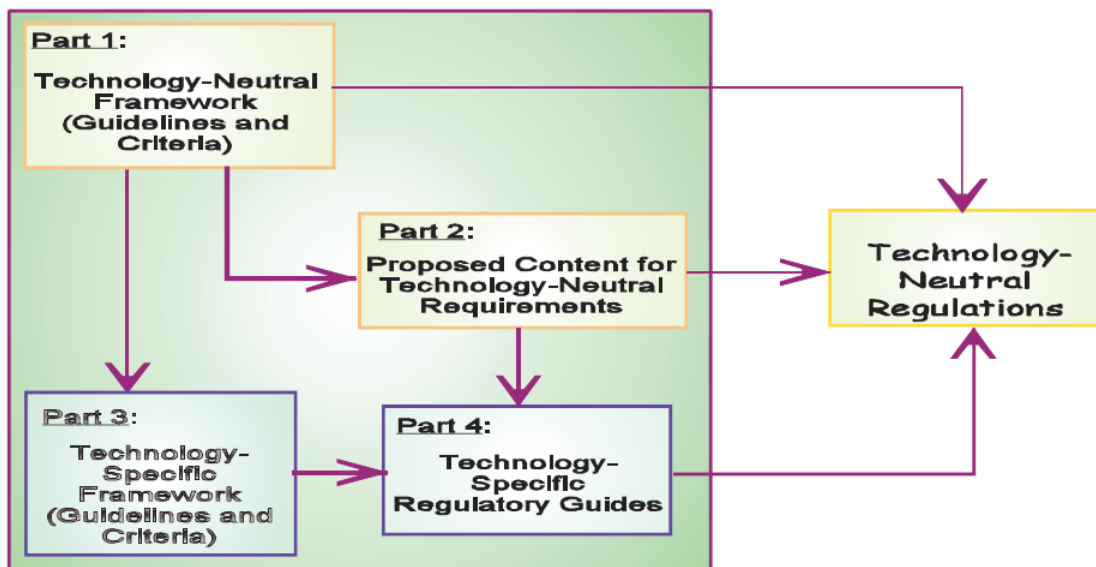


Figure 0-1 Framework for a Regulatory Structure for New Plant Licensing

In this framework and as discussed further by Delaney (2005), the NRC utilizes three main ideas to create a framework for risk-informed regulations:

- a hierarchical framework structure with the goal of protecting the public health and safety
- a balanced regulatory approach that maintains the philosophy of defense-in-depth
- quantitative guidelines based on these safety goals to define safety limits for advanced nuclear power plants.

The first concept is addressed by the notion of public risk objectives and defined by the Safety Goal Policy Statement of the NRC in terms of two quantitative health objectives (QHOs) (NRC, 2004):

- *“The risk to an average individual in the vicinity of a nuclear power plant of prompt fatalities that might result from reactor accidents should not exceed one-tenth of one percent (0.1 percent) of the sum of prompt fatality risks resulting from other accidents to which members of the U.S. population are generally exposed”.*
 - *The Commission defined “vicinity” in this case as the area within one mile of the plant site boundary, and the average individual risk is determined by the mean of the frequency-weighted early fatality distribution summed over all accidents and divided by the total population within 1 mile.*
- *“The risk to the population in the area near a nuclear power plant of cancer fatalities that might result from nuclear power plant operation should not exceed one-tenth of one percent (0.1 percent) of the sum of cancer fatality risks resulting from all other causes.”*
 - *The Commission defined the “area near a nuclear power plant” for this objective to be the area within 10 miles of the site boundary and the risk to the population was again stated in terms of average individual risk of latent cancer determined by the mean of the frequency-weighted latent cancer fatality distribution summed over all accidents and divided by the total population within 10 miles.*

QHO’s serve as very high level quantitative criteria that reactors must demonstrate they can meet. These criteria ultimately drive the determination of allowable limits when analyzing the risk of the considered design. The QHO’s appear to be reasonable in their intended purpose, however the methods to determine how a reactor concept meets these objectives through means of defense-in-depth and to identify quantitative design guidance remain immature and are a major aspect of this work.

1.2.1 Licensing of the PBMR

In the mid-80’s, a licensing approach of the Modular High Temperature Gas Reactor was developed for pre-application review by the NRC (DOE, 1992). This U.S. DOE-funded effort was carried out by several key gas-reactor contractors and utilized a top-down approach to licensing. In the early 90’s, Exelon Generation Company, under the support of outside

contractors, modified the approach for the PBMR and updated the effort to account for advancements in risk-informed regulation (Exelon, 2002). As discussed, the PBMR Group has a renewed interest in obtaining NRC licensing approval of the PBMR as well as some initial scoping efforts led by Areva regarding their high temperature reactor concept, AREVA-HTR. The licensing efforts for Exelon, Areva, and the PBMR Group were developed principally by Technology Insights, which was also actively involved in the initial DOE HTGR effort. A series of white papers developed for the NRC pre-application review of the PBMR (available on the NRC ADAMS web site) in addition to published papers (Silady, 2005; Fleming, 2005) provide a very thorough review of the licensing approach for the PBMR (US Design Certification, 2006). It should be noted that personal communication with Dr. Fred Silady of Technology Insights about the PBMR licensing approach was also invaluable. As discussed in later sections, the PB-AHTR shares substantial commonality with the PBMR and other HTR concepts and the PBMR licensing framework serves as an excellent starting point for the PB-AHTR (Peterson, 2008). Likewise, the differences between the PB-AHTR and these modular helium reactors help to illustrate how a generalized, technology-neutral licensing approach may be developed.

Key elements of this advanced reactor licensing strategy are reproduced below in Table 1. The key function that each element performs is also provided and facilitates the understanding of the overall licensing framework. The remainder of this section will provide an overview of each element. For further information, the reader is encouraged to review the series of white papers and literature discussed above.

Table 1 Modular HTGR Licensing Approach Elements (Silady, 2005)

Top Level Regulatory Criteria (TLRC)	Establish what must be achieved
Licensing Basis Events (LBE)	Define when the TLRC must be met
Regulatory Design Criteria (RDC) Safety Classifications of SSCs	Establish how it will be assured that the TLRC are met
Deterministic Design Conditions Special Treatment Requirements	Provide assurance as to how well the TLRC are met

1.2.1.1 Top Level Regulatory Criteria (TLRC)

The PBMR licensing strategy is a top-down approach starting from a clear set of TLRC which serve as standards for determining licensability of reactor concepts. As illustrated in Table 1, the TLRC answer the question of what level of safety must be achieved in the reactor concept for events of different frequencies. The TLRC proposed by the PBMR Group require specific safety levels that meet the two previously discussed QHOs. By developing a fundamental and quantitative basis in terms of acceptable potential radionuclide release, various nuclear

technologies can be evaluated by the same set of criteria. The PBMR licensing approach utilizes the same acceptable risk region approach outlined in the Technology-Neutral Framework (NRC, 2005). The so-called Farmer’s curve provides an acceptable region for risk by evaluating failure modes of a range of frequencies and consequences. The TLRC developed in the PBMR approach define this acceptable region for associated probabilistic and deterministic safety analyses and consist of existing NRC regulations, safety goals, and guidance (Figure 0-2).

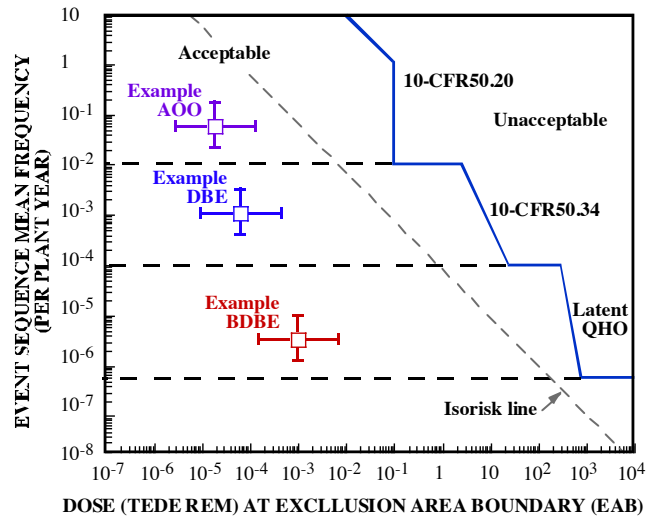


Figure 0-2 Relationship between event frequency and consequences for example event sequences, and comparison of consequences with TLRC limits for acceptable versus unacceptable consequences (US Design Certification, 2006).

In the acceptable region three categories of events based on their initiating frequencies. These event categories represent events that pose a different set of challenges to the plant and are listed below in order of decreasing event frequency:

- Anticipate Operational Occurrences (AOO)
- Design Basis Events (BDE)
- Beyond Design Basis Events (BDBE)

In existing LWR regulatory guidance the term accident is typically used instead of event (i.e. design basis accident). For the PBMR approach, a set of DBEs are examined and broken down into a smaller set of bounding licensing basis events (LBEs) that are examined in the licensing approach (Silady, 2005). This set of LBEs replaces the role DBAs played in the current LWR licencing structure and are discussed later in this section.

1.2.1.2 Licensing Basis Event Selection

As shown in Table 1, analysis of the consequences of different LBEs helps answer the question of whether the TLRC are met. For the design certification application (DCA) for the PBMR, a safety evaluation of a set of LBEs will be provided. While not every conceived transient can be

analyzed, a set of LBEs covering normal plant operation to rare BDBEs are analyzed to assess plant end states. Because only a subset of events is considered, the selection of LBEs must be done judiciously and must bound all potential operating modes of the reactor design. The equivalent set of DBAs in current NRC regulations includes challenging LWR transients such as loss of coolant accidents (LOCAs) which play a smaller role in many advanced reactor technologies. General design criteria (GDC) are codified in 10 CFR Part 50 Appendix A but are LWR-specific. The PBMR licensing approach introduces the idea of regulatory design criteria (RDC) to serve the role of the GDC, while the LWR GDC are reviewed for applicability to the PBMR and are then considered within the context of the RDCs. RDCs are discussed in greater detail next section.

The PBMR approach to LBEs is risk-informed and is based on both deterministic and probabilistic elements however rooted in deterministic engineering principles. The kinds of events, failures, and natural phenomena that are evaluated in the PBMR approach include:

- Multiple, dependent and common cause failures (CCF) to the extent that these contribute to LBE frequencies
- Events affecting more than one reactor system
- Internal events and internal and external plant hazards that occur in all operating and shutdown modes and potentially challenge the capability to satisfactorily retain radioactive material (i.e. earthquakes, hurricanes, tsunamis, tornados, etc.).

Selected LBEs represent a wide range of event frequencies categorized below by type. The NRC typically The frequency below which events are not selected as LBEs is 5×10^{-7} per plant-year. According to the Technology-Neutral Framework (2005), event sequences with a probability below 10^{-7} per plant-year (mean value) are considered extremely rare. At this extremely low frequency level events do not contribute to the QHO, and thus do not have to be considered in the design for licensing purposes (US Design Certification, 2006).

- AOOs – event sequences with mean frequencies greater than 10^{-2} per plant-year, that could occur during the life of a typical nuclear power plant.
- DBEs – event sequences with mean frequencies less than 10^{-2} per plant-year and greater than 10^{-4} per plant-year, that could occur during the lifetime of a family of around 100 reactors.
- BDBEs - event sequences with mean frequencies less than 10^{-4} per plant-year and greater than 5×10^{-7} per plant-year, that would be unlikely to occur in the lifetime of a family of around 100 reactors.

For the PB-AHTR, initiating events are identified using methods outlined in a Masters logic Diagram (Figure 0-3) and analyzed using PRA methods (discussed in the next section). By plotting all considered transients from the PRA on a frequency-consequence curve (Fig. 0-2),

event sequence families are identified. According to the PRA white paper (US Design Certification, 2006), event sequence families are used to group together two or more event sequences when the sequences have a common initiating event, safety function response, and end state. The following considerations were listed in the PBMR licensing documentation:

- “The guiding principle is to aggregate event sequences to the maximum extent possible while preserving the functional impacts of the initiating event, safety function responses, and end state. Note that for a multi-module plant, the end state includes the number of reactor modules involved in the event sequence.”
- “The safety function responses are delineated to a necessary and sufficient degree to identify unique challenges to each SSC that performs a given safety function along the event sequence. Event sequences with similar but not identical safety function responses are not combined when such a combination would mask the definition of unique challenges to the SSCs that perform safety functions.”
- “In many cases for a single module plant, there may be only one event sequence in the family.”
- “For a multi-module plant, event sequence families are used to combine event sequences that involve individual reactor modules independently into a single family of single reactor module event sequences.”
- “Each event tree initiating event and safety function response has a corresponding fault tree that delineates the event causes and SSC failure modes that contribute to the frequencies and probabilities of these events. Hence each event sequence is already a family of event sequences when the information in the fault trees is taken into account.”

1.2.1.3 Probabilistic Risk Analysis (PRA) Approach

The PRA method developed for the PBMR has been discussed extensively in the literature by Fleming (2005) and detailed in the PRA white paper (US Design Certification, 2006). According to the NRC webpage, current LWR PRAs are broken up into three distinct levels:

- Level I PRA - estimates the frequency of accidents that cause damage to the nuclear reactor core. This is commonly called core damage frequency (CDF).
- Level II PRA - which starts with the Level 1 core damage accidents, estimates the frequency of accidents that release radioactivity from the nuclear power plant.
- Level III PRA - which starts with the Level 2 radioactivity release accidents, estimates the consequences in terms of injury to the public and damage to the environment.

In the case of most advanced reactors where advanced fuel (i.e. TRISO) is used, the existence of a clear delineation between a Level I and II PRA is not appreciable because the fuel cannot melt. The PRA strategy for the PBMR is an integral approach characterizing event frequencies using traditional methods such as event trees and characterizing plant end states (i.e. consequences) in

the form of release categories. This quantification of frequencies and consequences of event sequences and the associated quantification of uncertainties provides an objective method of comparing the risk of different scenarios and of comparing safety performance against the TLRC (Silady, 2005).

PRA is used as a tool to help identify the LBEs in part due to its capabilities to account for the dependencies and dependencies and interactions among SSC, human operators and the plant hazards that may perturb the operation of the plant and lead to an accidental release of radioactive material. Rather than limit the quantification to point estimates of selected risk metrics, the PBMR PRA is structured to give emphasis to the treatment of uncertainties (US Design Certification, 2006). Due to the simplification of the overall design of the PBMR, the number of SSCs and events that need to be modeled is reduced. The reduction in complex active safety systems drastically simplifies the PBMR PRA model structure and allows for integral event sequence development spanning from the cause of the initiating event to the release category end state (Figure 0-4 Comparison of PBMR PRA with TLRC (Silady, 2005))

Table 2).

The PBMR approach to PRA uses a Master Logic Diagram in order to define the failure mode of each SSC and consequent impacts of each of these modes in challenging the barriers and safety functions. Two different paths are followed through the steps (Figure 0-3), one from the point of view of each barrier and its set of challenges, and the other from the point of view of the SSC providing safety functions in support of these barriers. The former may be viewed as direct challenges to the integrity of the barriers and the latter as indirect challenges to the barriers (US Design Certification, 2006).

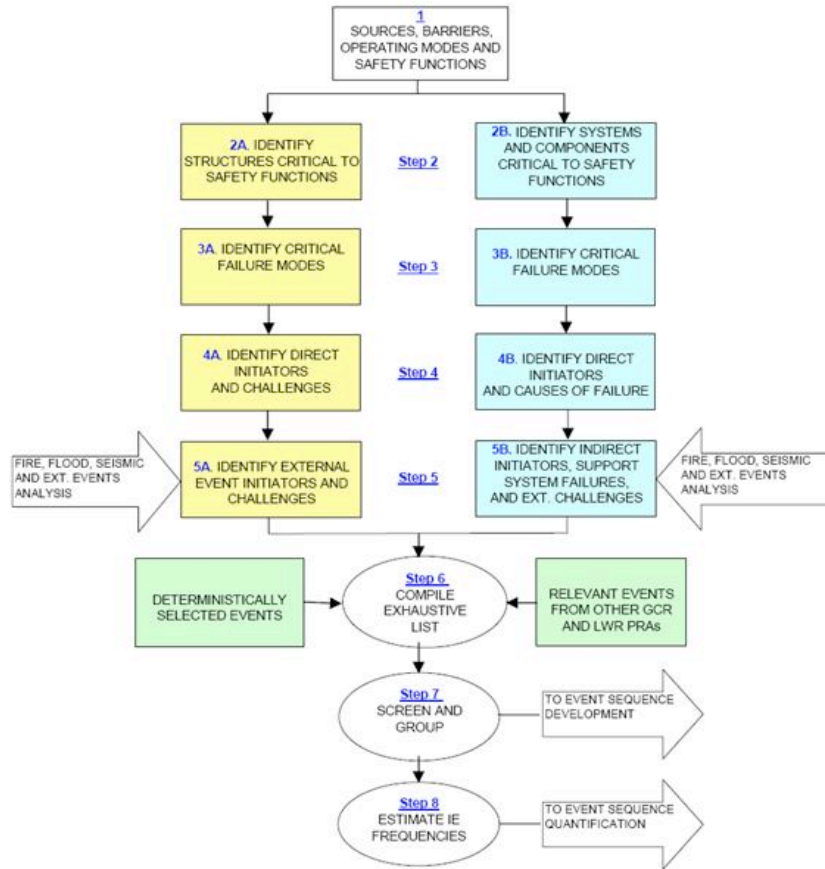


Figure 0-3 Master Logic Diagram for PBMR initiating events analysis (US Design Certification, 2006).

An event sequence modeling framework (**Error! Reference source not found.**) was used to structure the PRA approach and understand the accident evolution from initiation to end state. Ultimately, release categories are determined to describe reactor end state consequences for a range of events. It is acknowledged that the example release categories given will need to be validated using a range of fuel and system experiments. Each LBE is characterized in terms of event frequency and plant end state where it is evaluated against TLRC.

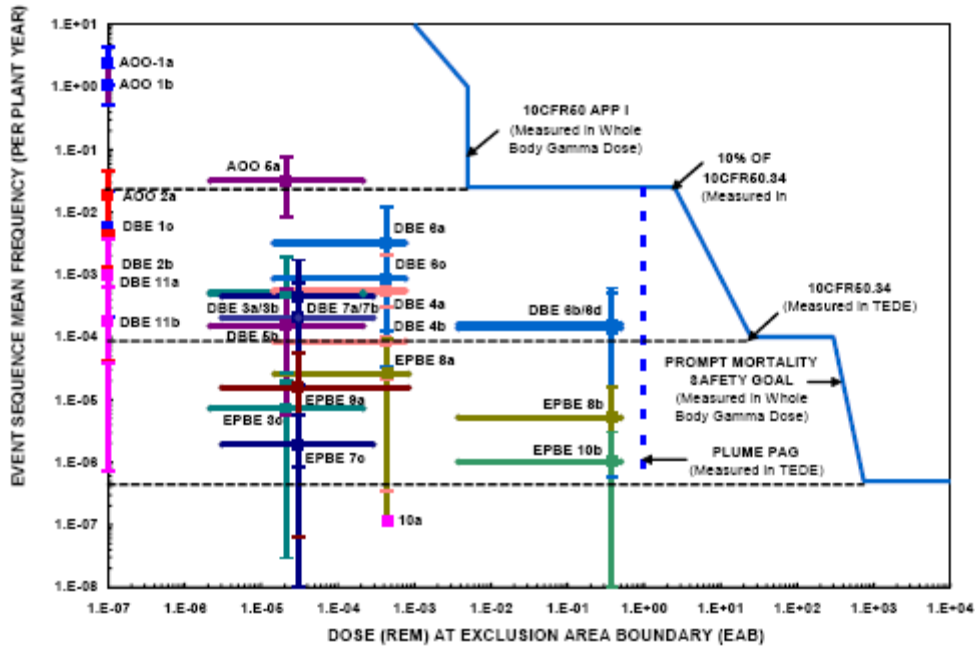


Figure 0-4 Comparison of PBMR PRA with TLRC (Silady, 2005)

Table 2 Example PBMR release categories (US Design Certification, 2006).

Code	Definition
RC-I	No release with an intact HPB
RC-II-F	Filtered release of all or part of circulating activity only
RC-II-U	Unfiltered release of all or part of circulating activity only
RC-III-F	Delayed filtered release from failed fuel with MPS pump-down
RC-III-U	Delayed unfiltered release from failed fuel with MPS pump-down
RC-IV-F	Delayed filtered release from failed fuel without MPS pump-down
RC-IV-U	Delayed unfiltered release from failed fuel without MPS pump-down
RC-V-F	Delayed filtered fuel release with oxidation from air ingress and lift-off of plated out radionuclides
RC-V-U	Delayed unfiltered fuel release with oxidation from air ingress and lift-off of plated out radionuclides
RC-VI	Loss of core, reactor vessel, or HPB structural integrity with unfiltered release

1.2.1.4 Regulatory Design Criteria and SSC Identification

Regulatory design criteria (RDC) are used to answer how the TLRC are met in the PBMR. RDC are written at a functional level to describe the requirements for SSCs needed during considered transients to assure compliance with 10 CFR Part 50 dose limits. The set of RDCs proposed for the PBMR are very similar in nature to the GDC found in Appendix A of the 10 CFR Part 50 but address HTR issues. Top level RDC categories for the PBMR and the transition from the existing GDC categories are shown in Figure 0-5.

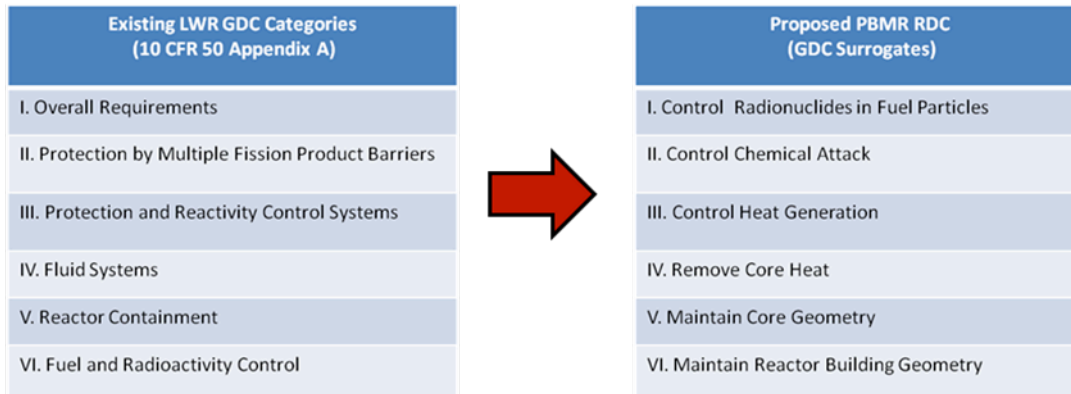


Figure 0-5 Transition from existing GDC categories to PBMR RDC categories

As discussed in the previous section, PRA is used to help determine RDC types. All existing GDCs were examined by the PBMR Group and evaluated for their specific relevance to the PBMR. The set of RDCs proposed are technology-specific to the PBMR and similar HTGRs but illustrates a shift in safety issues (transition from emphasis on LOCA analysis to chemical attack and fuel failure).

Because the question of how TLRC are to be met is answered by evaluating a set of RDCs, a methodology for classifying equipment as safety-related was developed based on SSCs that are relied upon to ensure that event consequences are within acceptable design basis limits. The PBMR licensing approach proposes a two step process to identifying SSCs as safety related (Silady, 2005):

- Step 1: Consequence Mitigation: SSCs that are relied upon to meet DBE dose acceptance criteria are classified as safety-related for each DBE
- Step 2: High-Consequence Prevention: SSCs that are relied upon to assure event frequency remains below the lower bound frequency limit (DBE region) for each BDBE with consequences greater than that specified in 10 CFR Part 50.34(a) are safety related

Required safety functions in the first step must be performed over the full spectrum of DBEs considered in the PRA to ensure TLRC is not violated. In the second step, an independent check is performed to ensure that the set of safety-related SSCs is complete. The role of SSCs is discussed further in the next section on defense in depth.

1.2.1.5 Defense-in-Depth Treatment

The PBMR licensing approach towards defense-in-depth is heavily reliant on the inherent and passive characteristics of SSCs in carrying out their specified safety functions required to prevent and mitigate design basis events. According to the PBMR white paper on defense in depth (2006), "... this approach of providing combinations of inherent features and passive SSCs to perform the required safety functions as well as additional redundant and diverse active SSCs to perform these same functions is strong evidence of a robust approach to defense-in-depth".

Defense-in-depth was also applied in the overall safety evaluation process for the PBMR. The use of conservative assumptions and the approach to treating uncertainties throughout the licensing process is considered a form of defense-in-depth. A formal method for objective quantitative evaluation of the roles that specific SSCs play in defense-in-depth is documented in the white paper and is based on meeting different levels of defense by risk-informed evaluation, plant capability, and programmatic implementation. The reader is directed to the aforementioned resources for more information on the PBMR approach to defense in depth depicted in Figure 0-6.

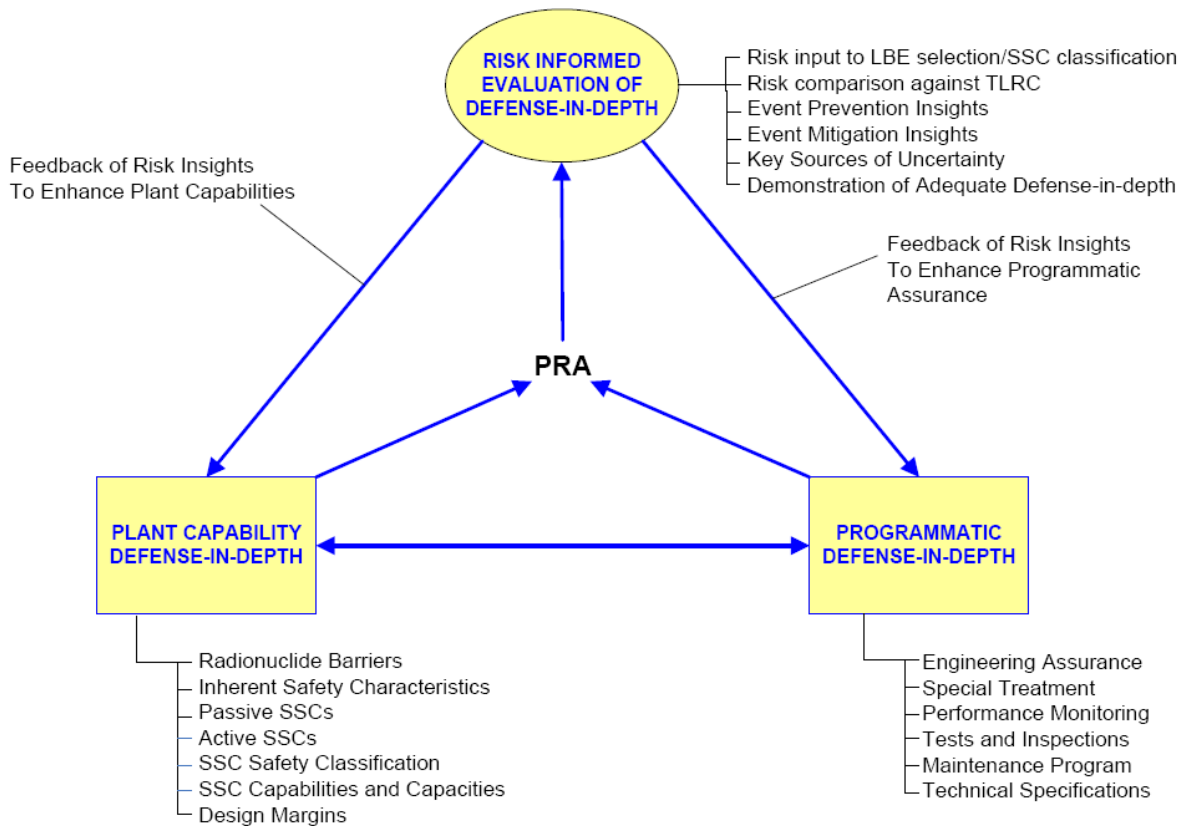


Figure 0-6 Detailed elements of PBMR approach to defense-in-depth (US Design Certification, 2006)

2 Case Study: Modular PB-AHTR Reactivity Control

2.1 PB-AHTR Overview

The Pebble Bed Advanced High Temperature Reactor (PB-AHTR) is a liquid-salt cooled, high temperature reactor design developed at UC Berkeley in collaboration with Oak Ridge National Laboratory. The PB-AHTR is the latest design based on the original AHTR concept to use liquid fluoride salt to cool coated particle high temperature reactor fuels (Ingersoll et al., 2004), which has undergone several transformations over the last 4 years (Peterson et al., 2008). The PB-AHTR takes advantage of technologies developed in gas-cooled high temperature thermal/fast reactors, sodium fast reactors, and molten salt reactors. The modular 900-MWth PB-AHTR is the reference design for this case study (Bardet et al., 2008).

In **Error! Reference source not found.**, the primary loop of the PB-AHTR is represented by the blue line connecting the core and the Intermediate Heat exchanger (IHX) modules. During a loss of forced circulation (LOFC) transient (i.e. after a primary pump trip), a natural circulation flow loop is formed between the core and a set of Direct Reactor Auxiliary Cooling System (DRACS) heat exchangers (DHX modules), as indicated by the purple flow path. The DRACS heat exchangers transfer heat by natural circulation flow of a DRACS salt from the DHX modules to heat rejection exchangers cooled by outside ambient air. Under forced circulation the reverse bypass flow through the DHX is minimized by a fluidic diode. The annular space between the reactor vessel and the guard vessel is filled with a low-cost buffer salt, a mixture of sodium and potassium fluoroborate, which minimizes primary salt inventory loss if the reactor vessel is faulted. The red flow path represents the IHX's secondary loop which can be used to deliver thermal power to a variety of applications such as process heat for hydrogen generation or electricity generation in addition to other power co-generation options.

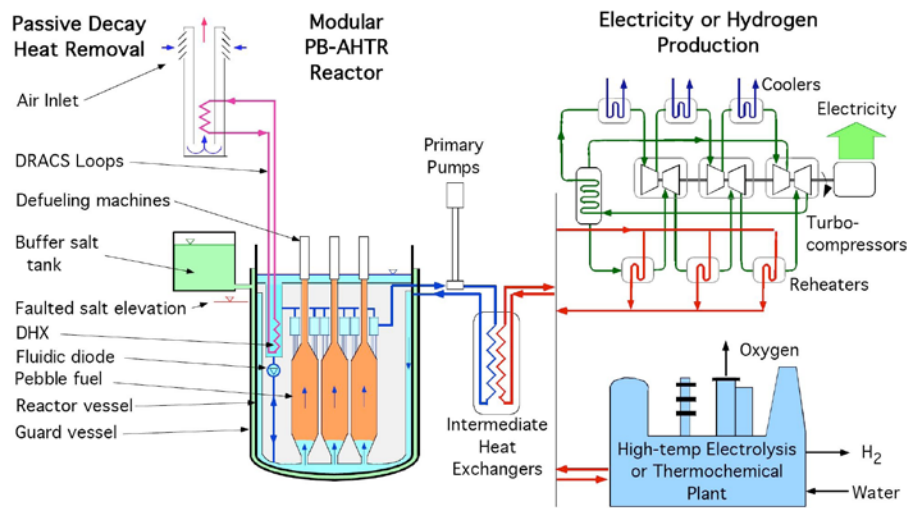


Figure 0-1 Simplified schematic of modular PB-AHTR system and possible applications

As mentioned previously, the modular PB-AHTR shares substantial commonality with other advanced reactor technologies. However some key design differences make the PB-AHTR attractive economically, in particular with respect to high-temperature gas reactors (HTGR). Key design differences and a comparison of operating parameters of the PB-AHTR and leading HTGR designs are listed below in Table 3 and Table 4.

Table 3 Comparison of Key Design Differences

Design Feature	GT- MHR	PBMR	PB-AHTR
Core configuration	Prismatic core consisting of fuel elements containing compacts	Pebble bed	Pebble Channel Assemblies
Core diameter (m)	2.96 ID/ 4.83 OD	2 ID/3.7 OD	0 ID/3.75 OD
Effective Core Height (m)	7.93	8.5	3.2
Core thermal-hydraulics	Flow channels in fuel elements	Flow paths through porous pebble bed	Flow paths through porous pebble bed channels
Passive cooling	Air-cooled Reactor Cavity Cooling System (RCCS)	Air-cooled Reactor Cavity Cooling System (RCCS)	Air-cooled DRACS

Table 4 Comparison of Nominal Full Power Operating Parameters

Nominal full power operating parameters	GT- MHR	PBMR	PB-AHTR
Reactor power (MWt)	600	400	900
Core inlet/outlet temperature (°C)	491/850	495/890	600/704
Core average temperature (°C)	670	692	652
Core inlet/outlet pressures (MPa)	7.07/7.02	7.0/	0.7/0.0
Primary mass flowrate (kg/s)	320	140	3,625
Turbine(s) inlet/outlet pressures (MPa)	7.0/2.6	7.0/2.6	10.0/5.7/3.2/1.8
Turbine(s) inlet/outlet temperature (°C)	848/511	751/554	675/495
Core Power density (MWth/m ³)	~ 5	~ 6.6	~20-30
Net electrical output (MWe)	286	165	410
Net plant efficiency(%)	48	41	46

2.1.1 Key Safety Features

A list of the key safety systems for the PB-AHTR is below in Table 5 and distinguished by type (active vs. passive). A description of each safety feature and related safety function is also given.

Table 5 Key safety features of the modular PB-AHTR

Safety System	Type	Related Safety Function	Description
Fuel	Passive Type A	Maintain control of radionuclides Provide thermal inertia	The TRISO fuel is designed to confine radioactive materials up to high temperatures. The graphite in the fuel provides thermal inertia. Failures can occur due to fabrication methods and high temperature operation.
PCA and Reflectors	Passive Type A	Provide thermal inertia	The PCA and reflectors are made of large amounts of reactor-grade graphite and are capable of providing high thermal inertia during transients.
Primary coolant	Passive Type B	Provide thermal inertia Heat removal Maintain control of radionuclides	The primary coolant has a high volumetric heat capacity and is capable of removing large amounts of heat at lower flow rates. The flibe also is effective in absorbing and confining fission products.
Shutdown rod system	Passive Type A,B,&D	Suppress reactor flux during transients	The shutdown rod system is designed to operate in both active and passive modes completely independent of each other.
Primary system boundary	Passive Type A	Maintain control of radionuclides Preserve primary loop geometry	The primary system boundary contains the primary salt and its cover gas, and provides a barrier to confine fission products.
Reactor cavity	Passive Type A	Maintain control of radionuclides Heat removal	The reactor cavity provides low-leakage, low pressure containment of fission products, and is insulated had has a heating system to control heat losses to prevent freezing of the primary salt.
Reactor citadel	Passive Type A	Maintain control of radionuclides	The reactor citadel structure provides maintenance space for primary loop equipment and provides a low-pressure filtered confinement for fission products.
Reactor building and turbine hall	Passive Type A	Maintain control of radionuclides Preserve geometry of reactor citadel	The reactor building and turbine hall provide an external events shell for the reactor citadel, and provide additional hold up and confinement of fission products.
DHX	Passive Type A & B	Heat removal	Provides natural-circulation heat removal to air cooled heat rejection heat exchangers for decay heat removal, and acts as a portion of the primary system boundary
IHX	Active	Heat removal	Provides forced circulation heat removal to the power conversion system, and natural circulation heat removal to the shutdown cooling system, and acts as a portion of the primary system boundary

2.1.2 State of Technology

Recent studies of the PB-AHTR have addressed key viability issues: (1) experimental studies with the Pebble Recirculation Experiment (PREX-1), shown in Figure 0-2, have demonstrated pebble bed generation and pebble recirculation with liquid salts (Bardet et al., 2007), (2) RELAP5-3D modeling of Loss of Forced Circulation (LOFC) transients has verified the capability to operate at high power density compared to helium cooled PBMRs (Griveau, 2007), and (3) neutronics studies have verified the capability to design LEU and deep-burn TRU cores with negative temperature and void reactivity feedback, and to achieve high fuel discharge burn up levels (Zwan, 2007; Fratoni, 2007).

2.1.2.1 Experimental Work

The Pebble Recirculation Experiment (PREX-1), shown schematically in Figure 0-2, is a scaled model of the original 2400 MWth AHTR-MI core and was developed to demonstrate the feasibility of pebble injection, recirculation, and defueling in liquid-salted cooled beds. PREX takes advantage of the fact that water can be used to simulate the hydrodynamics of the liquid salt flibe (Bardet et al, 2006). To reproduce the hydrodynamic behavior of pebbles in liquid flows, the drag and buoyancy force on the pebbles must be matched. This gives rise to the ratio of terminal velocity of the pebble. Hence, for pebbles dynamics scaling, the Reynolds number, Froude number and pebbles to fluid densities ratio must be matched,

$$\frac{V_p^{\infty 2}}{U^2} = \left(\frac{4}{3} \left(1 - \frac{\rho_p}{\rho_f} \right) \frac{1}{C_D Fr} \right)$$

Where ρ_p and ρ_f are pebble and fluid densities, C_D is drag coefficient and, Fr , is the Froude number, $Fr = U^2/d \cdot g$. In the Froude number, d is pebble diameter and g acceleration of gravity. Reynolds number based on the pebble diameter is introduced in the terminal velocity through the drag coefficient, $Re_p = V_p d / \nu$. In this equation, V_p is the pebble differential rise velocity with respect to the fluid velocity.

2.1.2.2 Computational Modeling Efforts

Recent UC Berkeley RELAP5-3D studies by Griveau et al. (2007) found that the initial selection of 10.2 MW/m³ power density for the AHTR appears to be conservatively low (although 10.2 MW/m³ is over twice the typical 4.8 MW/m³ power density of the PBMR). These studies encouraged UCB to shift its experimental and modeling work to examine a 900-MWth modular



Figure 0-2 Scaled PREX-1 experiment

PB-AHTR design with a power density in the range of 20 to 30 MW/m³. The resulting conceptual design has 50% greater power output and the same 46% power conversion efficiency as the 600 MWth GT-MHR, but with a low-pressure reactor vessel that is 1/10th the volume of the 70-atm GT-MHR vessel.

2.3 Description of PB-AHTR Reactivity Control System (RCS)

In the PB-AHTR, reactivity is controlled by the reactor control system (RCS) during normal or expected operation. As required by GDC 26 in 10 CFR Appendix A to Part 50, the PB-AHTR is required to have two independent reactivity control systems with different design principles. The PB-AHTR has the following reactivity control methods, (1) Normal shutdown by forced insertion of the 6 shutdown rods by the reactivity operational controls system (ROCS) or by operator action; (2) Reserve shutdown by insertion of the 32 control rods by the reactivity protection system (RPS) or by operator action; (3) Reserve shutdown by passively driven buoyancy-activated insertion of the 6 safety rods; and (4) shutdown by core negative temperature feedback. Elevation and plan views of the PB-AHTR depicting the locations of the control and shutdown safety rods can be found in Figure 0-3. Following a scram signal or other shutdown signal, the shutdown rods and control rods are inserted via gravity insertion by a heavy control rod actuator located above the rod when the power is cut to the actuation mechanisms for both systems. For reserve shutdown, the shutdown rods will also insert passively due to negative buoyancy resulting from the rise of coolant temperature. One of the primary focuses of this work is to quantify the efficacy of the buoyancy-driven shutdown rod and overall reliability of buoyancy-activated shutdown with respect to other reserve shutdown options. A summary of the diverse reactivity control systems in the PB-AHTR is listed in Table 6 and a general logic diagram indicating the different levels of defense is provided in Figure 0-4.

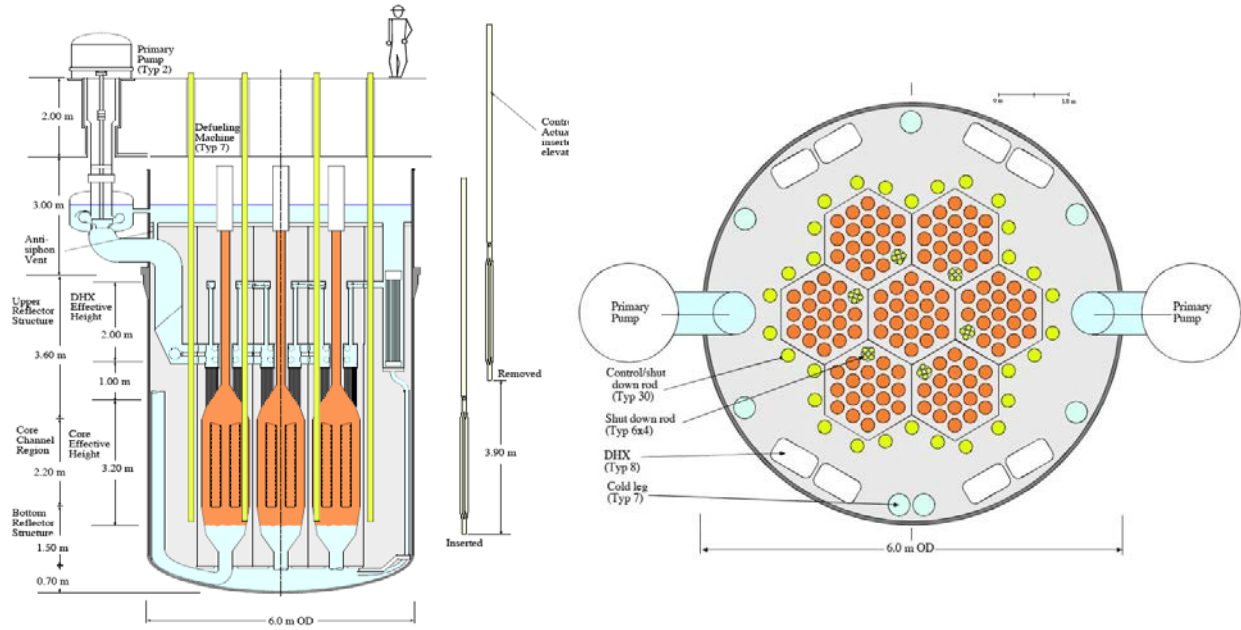


Figure 0-3 Elevation and plan view showing shutdown rod in fully inserted position

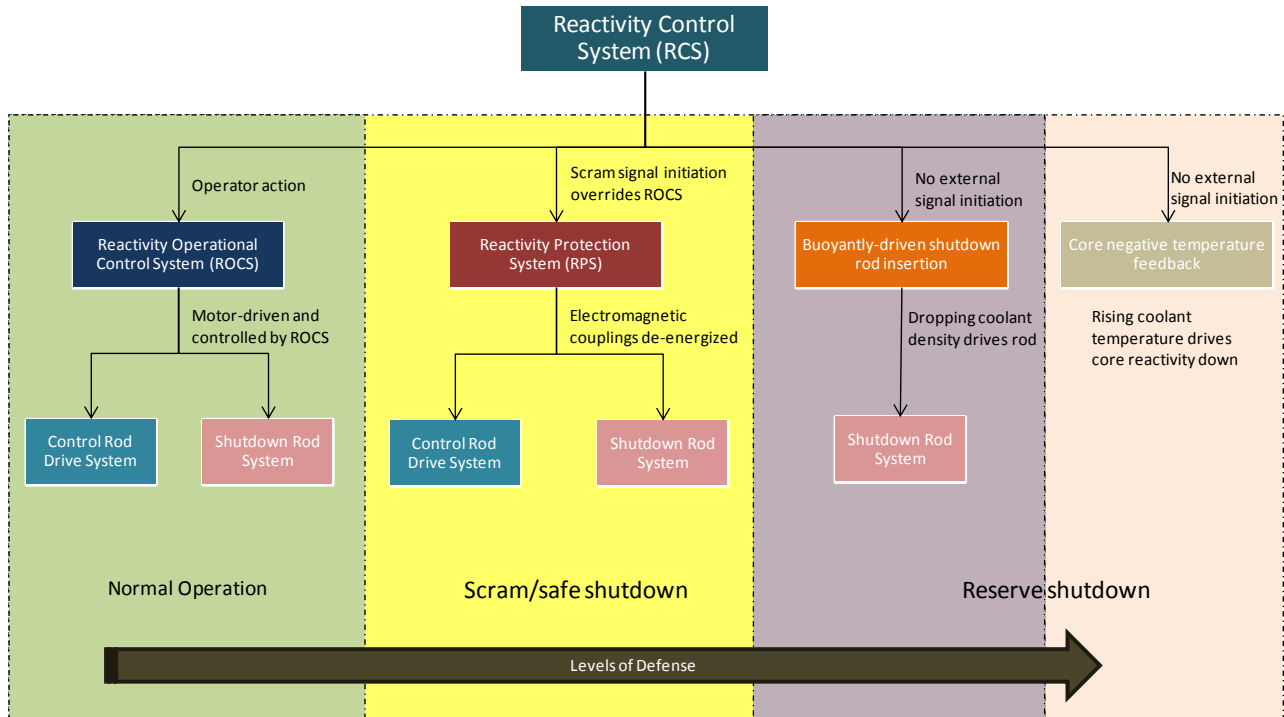


Figure 0-4 General logic diagram of PB-AHTR reactivity control system

Typically for HTGRs, a Small Absorber Sphere (SAS) system is used for reserve shutdown. In the PB-AHTR the role of the SAS has been replaced with a buoyancy-driven reserve shutdown system. The injection of a soluble neutron poison (sodium fluoroborate salt) has also been considered as a reserve shutdown mechanism, but the buoyancy-activated shutdown rod system is considered preferable due to its intrinsic passive activation method, its simpler phenomena (injection, dissolution, and transport of sodium fluoroborate all involve complex phenomena), and its reduction of potentially costly inadvertent activation events.

Table 6 Summary of diverse PB-AHTR reactivity control systems in addition to intrinsic core negative temperature feedback

Reactivity Control System	Shutdown Rod System			Control Rod Drive System	
<u>Control Element</u>					
Number	6			32	
Material	B ₄ C			B ₄ C	
Density (kg/m ³)	1,980			TBD	
<u>Drive</u>					
Mode	Active	Active (scram)	Passive	Active	Active (scram)
Power Supply	ROCS	RPS	None	ROCS	RPS
Motor	Slow speed, stepping motor	None	None	Constant speed DC motor	None
Trip Insertion	Actively lowered into the core	Magnet release, gravity-driven	Buoyancy-driven	Power driven insertion	Magnet release, gravity-driven
Trip Snubber	None required	Actuator arresting device and rod hydrodynamic snubber	Hydrodynamic snubber	None required	Arresting device
<u>Performance</u>					
Trip insertion times					
Core midplane	6.2	0.6 s	TBD	8 s	8 s
Full insertion	9.4	0.9 s	TBD	12 s	12 s

2.3.1 Reactivity Control and Protection System Functionality and Modes of Operation

During normal operation, the RCS must be able to position both shutdown and control rods at any location in the core. This function is achieved using the ROCS which is responsible for initiating the shutdown rod driving mechanisms (see Figure 0-5 for a schematic of both systems

drive mechanisms). During a scram signal, the RPS overrides the ROCS and cuts electrical power to the electromagnetic coupling between both drive mechanism and heavy element causing both shutdown and control rods to insert by gravity taking a predetermined amount of time. The motions of both types of rods' motion are snubbed by a arresting devices located below both active driving mechanisms. For the case of the safety rod which is not mechanically coupled to the actuating drive element, the downward motion of the safety rod is snubbed by a hydrodynamic arresting channel at the bottom of the safety rod channle (**Error! Reference source not found.**) which uses a unique geometry to generate significant fluid forces to rapidly dissipate the rod's kinetic energy.

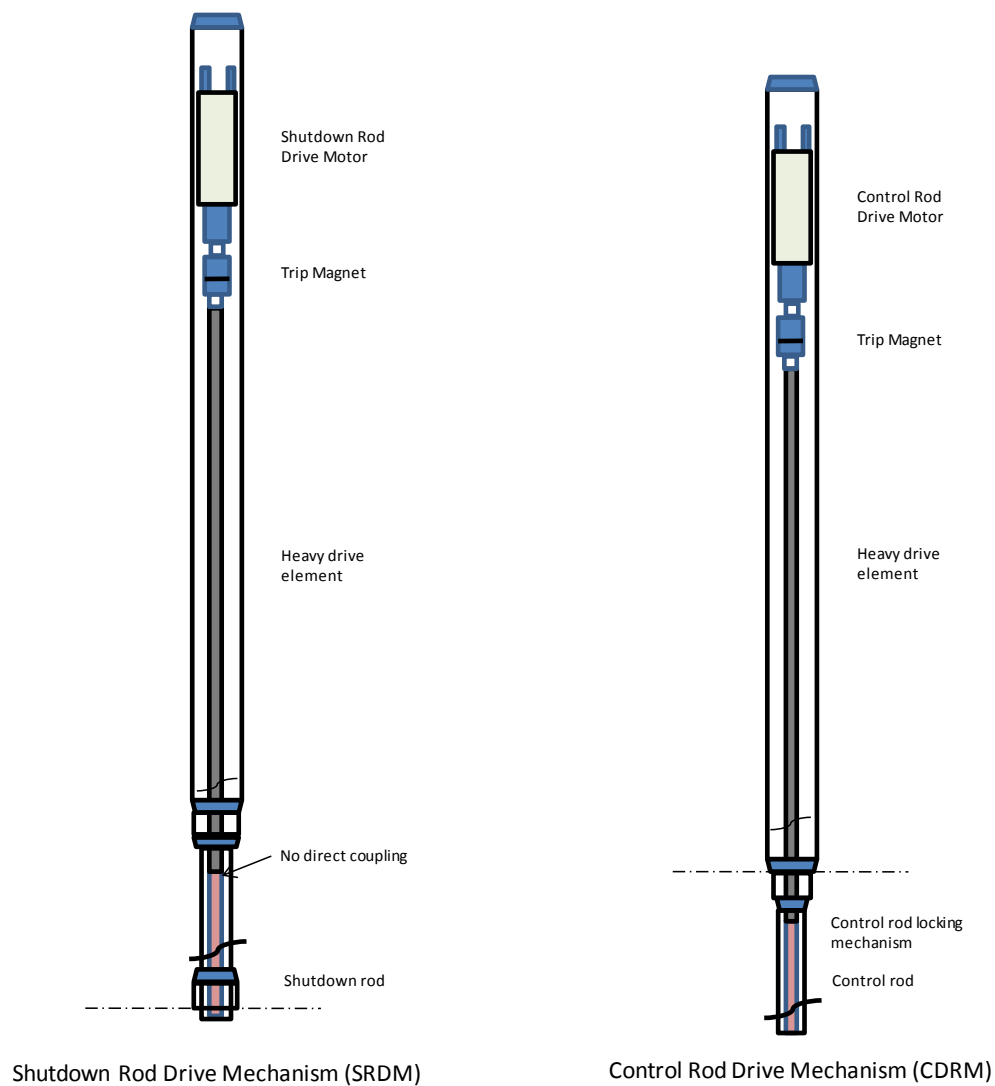


Figure 0-5 Schematic of RPS diverse drive mechanisms for rod insertion; (a) SRDM and (b) RCDRM

For both the SRDM and the CDRM, under the current baseline design drive motors are used to position the SRS and CRDS respectively. The SRS and CRDS are only in the preliminary design phase but their functional requirements are well understood. The actual design of the control rod is still being determined, however the initial design of the shutdown rod (but not the actuator drive element) has been completed. Each drive mechanism is controlled by the RCS Control and Instrumentation (C&I) system. A more detailed analysis of the performance and long-term reliability of the RCS is provided in Chapter 5.

HTGRs, such as the GT-MHR and PBMR, utilize separate shutdown and reserve shutdown elements (rod and sphere insertion) whereas the PB-AHTR baseline design uses the same shutdown element but different driving mechanisms (buoyancy and electro-magnetically activated forced insertion). However from a risk perspective, the type of event that would disable the passively driven shutdown rod system buoyancy-activated insertion would be one that disrupted the overall channel geometry of the insertion channel. In the PBMR a similar event is possible where the central reflector geometry could be disrupted, and this type of common-mode event would affect both the rod and sphere insertion systems (however, it is acknowledged that due to the small diameter of the spheres the risk is lower). In these cases, in both types of reactors reactivity shutdown would then occur from negative temperature feedback.

2.3.1 Buoyant Shutdown Rod Concept

The PB-AHTR implements a novel buoyant shutdown rod design for passive insertion of its shutdown rod elements to provide this negative temperature feedback to augment the negative feedback already provided by the negative coolant and fuel temperature reactivity coefficients. Insertion of the shutdown rods occurs due to buoyancy forces generated by the difference between the density of the control element and the reactor coolant.

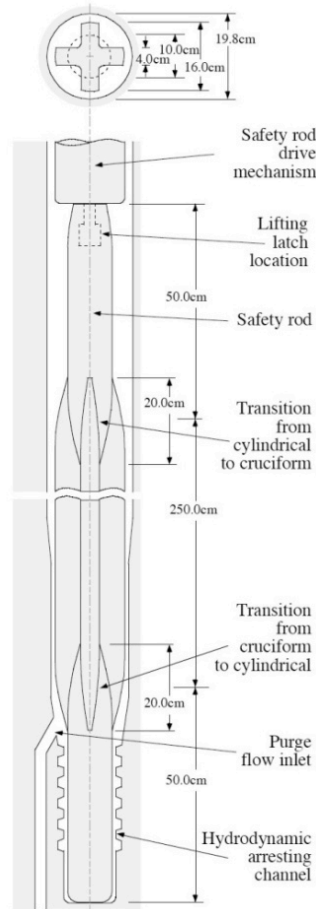


Figure 0-6 Buoyant shutdown safety rod design

Under normal steady-state forced circulation operation, a purge flow is metered into the bottom of each shutdown channel by a fluidic diode. The purge flow comes from the core inlet plenum, at the core inlet temperature $T_{ino} = 600^{\circ}\text{C}$. The purge flow results in an average upward coolant flow velocity in the channel U_{co} of approximately 0.2 m/s. The purge flow is expected to be metered by a fluidic diode, so that reverse flow after the primary pumps shut down in a LOFC transient has low flow resistance. The shutdown rods are located in 19.8-cm diameter shutdown rod channels (SRC) in six of the seven hexagonal Pebble Channel Assemblies that comprise the PB-AHTR reactor core, as shown in Figure 0-3. Each of the shutdown rods is designed to be neutrally buoyant at a flibe salt density corresponding to a flibe temperature of $615^{\circ}\text{C} \pm 5^{\circ}\text{C}$, taking into account all sources of uncertainty in the safety rod buoyancy (as identified in the preliminary PIRT study in Section 4.5). The shutdown rods can be comprised of a number of separate elements, composed of graphite and boron carbide, and linked together in a chain by a metallic or carbon composite rod tensioned by a spring.

There are two primary transients which generate scram signals to insert the shutdown elements: Loss of Forced Circulation (LOFC), where the primary pumps stop, and Loss of Heat Sink (LOHS), where heat removal is interrupted from the intermediate heat exchangers (IHX's), but

the primary pumps continue to operate. Each of these transients generate a number of changes that can be measured by temperature, pressure and motor current instrumentation, which in turn can be used to generate control signals to trip the primary pumps and scram the reactor (e.g., interrupt the electrical current to the magnetic latches for the shutdown and control drive elements). Additional control signals, for example from manual scram buttons in the control room and from seismic acceleration sensors, can also generate scram signals. Section 4.5.4 describes the system response during both transients.

The RCS is designed to have very high reliability to generate scram signals under LOFC and LOHS transients but some finite probability exists that these signals would not be generated, and that the magnetic latch and shutdown drive mechanisms would not function appropriately. Under these low-probability conditions, the shutdown drive elements would still respond to buoyancy forces generated due to the changing temperature of the coolant in the shutdown channels. Even if the shutdown and control drive elements do not function at all, under LOFC and LOHS transients the negative fuel and coolant temperature reactivity feedback causes the reactor power to drop as these temperatures increase during the transient. The role of the buoyantly-driven shutdown elements is to provide additional negative coolant temperature feedback, to reduce the peak core outlet temperature reached during the transient, and to provide effective shutdown of the reactor and greatly delay any re-criticality.

From a risk perspective, the two biggest questions are how the SRS will perform following different types of initiating events (i.e. insertion velocity and time) and how reliable will the system be over the duration of the plant's lifetime. In order to first understand how the SRS performs, a phenomenological model describing the rod dynamics must be developed to predict performance under buoyantly driven insertion. Subsequently, an experimental program is required to validate the analytical model and assess performance.

2.3.1.2 Forces Acting on Safety Rod

The forces acting on the control element include coolant drag on the safety rod, the weight of the safety rod, and the buoyancy force acting on the safety rod. A schematic of the forces acting on the safety rod and key geometry parameters is shown in Appendix A. These forces and potential sources of uncertainty are discussed in the following sections. The theory for an analytical model describing the shutdown rod response is presented in Appendix A and discussed further in Section 4.3.2.

Coolant Drag

During steady-state and transient operation, coolant drag forces act on the safety rod in the same direction of the coolant flow. Coolant drag is the sum of the form drag and skin friction drag. Expressions for the overall coolant drag are discussed below.

Form drag:

Form drag is a strong function of the cross-sectional area and general shape of the control element. To reduce form drag, a designer can use more streamlined shapes. Form drag can be calculated using the following expression where C_D and A_{cs} are the drag coefficient and maximum cross-sectional area respectively.

$$F_{sd} = \frac{1}{2} C_D \rho_{fluid} A_{cs} v_{fluid}^2$$

The form drag force is a strong function of the drag coefficient which can be determined experimentally or found in reference sources for common shapes. Since the safety rod consists of a crucifix section and two cylindrical sections, the total form drag force on the element is the sum of the drag forces acting on each section. Drag coefficients for the cylindrical and crucifix sections are taken from tabulated data [Ref X] and values of 0.5 and 0.2 are used respectively. Therefore, the total drag force on the safety rod is determined below where ρ_{flibe} and v_{avg} are the density and average channel velocity of the flibe respectively.

$$F_{fd} = \frac{\rho_{flibe} v_{avg}^2}{2} (C_{D,cr} A_{cr} + C_{D,cyl} A_{cyl})$$

It is important to note that the flibe temperature, density and velocity will change over the course of a transient, therefore affecting the form drag force acting on the control element modestly. The transient safety rod response model accounts for this effect and is discussed further in Appendix C.

Viscous drag:

Viscous drag, or skin friction drag, is caused by the shearing force of the fluid on the element within the momentum boundary layer. In order to calculate the viscous drag force acting on the safety rod, the shear stress the flibe acts on the element must first be determined. For turbulent flow conditions, the shear stress at the wall can be estimated using the following relationship where v_l and Re_l are the local velocity and local Reynolds number respectively.

$$\tau = \frac{1}{8} f_v \rho_{fluid} v_l^2$$
$$f_v = 0.316 Re_l^{-0.25}$$

The local velocity and Reynolds number can be assessed assuming continuity through the channel where A_{ch} , A_{cyl} , and A_{cr} are the cross-sectional areas of the channel, cylindrical sections and crucifix section respectively. The local Reynolds numbers are calculated using the hydraulic diameters of the flow near the crucifix (cr) and cylindrical (cyl) sections (Figure 0-1).

$$v_{cyl} = v_{avg} \left(\frac{A_{ch}}{A_{ch} - A_{cyl}} \right), \quad v_{cr} = v_{avg} \left(\frac{A_{ch}}{A_{ch} - A_{cr}} \right)$$

$$\text{Re}_{cyl} = \frac{v_{cyl} D_{h,cyl}}{v_{flibe}}, \quad \text{Re}_{cr} = \frac{v_{cr} D_{h,cr}}{v_{flibe}}$$

Combining the above relationships, the viscous drag force can be determined by multiplying the shear stress by the affected area.

$$F_{vd} = \tau_{cyl} \cdot A_{cyl_s} + \tau_{cr} \cdot A_{cr_s}$$

$$F_{vd} = \frac{0.316}{8} \rho_{flibe} \left(\text{Re}_{cyl}^{-0.25} v_{cyl}^2 A_{cyl_s} + \text{Re}_{cr}^{-0.25} v_{cr}^2 A_{cr_s} \right)$$

During a transient, it is important to note that the above expression is dependent upon both the density and the velocity of the flibe during the event of interest. Similar to the form drag, the transient safety rod response model will account for these effects and is discussed further in Appendix C.

Combining the form and viscous drag, the total drag force acting on the safety rod is expressed below. Since the velocity increases in the reduced area surrounding the shutdown rod, v_{cr} and v_{cyl} are the velocities near the crucifix and cylindrical elements respectively. The approach velocity for the form drag is just the average flow velocity in channel near the rod (v_{avg}).

$$F_D = F_{fd} + F_{vd}$$

$$F_D = \frac{\rho_{flibe}}{2} \left[v_{avg}^2 (C_{D,cr} A_{cr} + C_{D,cyl} A_{cyl}) + \frac{0.316}{4} \left(\text{Re}_{cyl}^{-0.25} v_{cyl}^2 A_{cyl_s} + \text{Re}_{cr}^{-0.25} v_{cr}^2 A_{cr_s} \right) \right]$$

Buoyancy Force on Safety Rod

The buoyancy force on the safety rod is a function of the volume of the element and densities of both the element and the flibe. The forces are acting in opposite directions and an expression for the difference is below. It should be noted that the calculation for the volume of the shutdown rod is only approximate as there are shape transitions between the cylindrical and crucifix elements.

$$F_B - F_W = V_{rod} g (\rho_{flibe} - \rho_{rod})$$

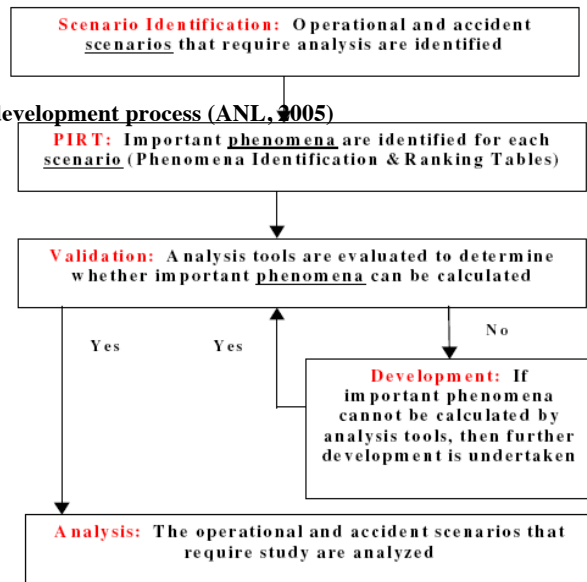
$$V_{rod} = 2 \cdot A_{cyl} \cdot L_{cyl} + A_{cr} \cdot L_{cr}$$

3 Phenomena Identification and Ranking

3.1 PIRT Procedure

In September 1988, the NRC issued a revised emergency core cooling system (ECCS) rule (USNRC, 1988) for light water reactors that allows, as an option, the use of best estimate (BE) plus uncertainty methods in safety analysis. The key feature of this licensing option relates to quantification of the uncertainty in BE safety analysis and inclusion of this uncertainty in the determination that a nuclear power plant has a ‘low’ probability of violating the safety criteria specified in 10 CFR 50. To support the 1988 licensing revision, the NRC and its contractors developed the code scaling, applicability and uncertainty (CSAU) evaluation methodology to demonstrate the feasibility of the BE plus uncertainty approach (Boyack et al., 1990).

Figure 0-1 R&D development process (ANL, 2005)



In Figure 0-1, the role of the PIRT process in the overall BE licensing effort is illustrated. The role of PRA is integral in assessing the range of scenarios that must be considered for the PB-AHTR. The PIRT process is used to prioritize the associated phenomena and help the designer understand where to focus R&D efforts and represents just one step of the CSAU methodology. For the PB-AHTR, RELAP5-3D is used to model transients under a range of operating conditions. This work will ultimately help verify RELAP system analyses of the PB-AHTR by providing realistic rod worth curves for a range of transient simulations following a structured approach using CSAU methods. While simulation of the actual response of the rod would require a coupled thermal-hydraulic and neutronic analysis (i.e. rod falling will suppress the reactor power and change the coolant temperature), this initial conservative approach to modeling the shutdown rod response serves the main purpose of proof-of-principle modeling and overall reactivity shutdown system efficacy determination.

3.1.1 Application of PIRT to Shutdown Rod System Response

In order to perform a PIRT study on the shutdown rod system, a key set of nucleus events must be selected. These events represent a range of operating conditions for the particular component or system under consideration. This preliminary PIRT focuses solely on the PB-AHTR shutdown rod system and considers two highly-ranked event scenarios and an expected reactivity shutdown event: LOFC, LOHS, and safe shutdown following IHX tube rupture (AOO). The forces acting on the shutdown rod were discussed in Section 4.3.1.2 and are very well understood assuming no change in shape geometry (drag and buoyancy forces are strong functions of flibe velocity and density respectively). The key focus of this PIRT study is to develop a better understanding of the range of operating conditions for the shut down rod system and subsequently the integrated response of the system. For more examples of PIRT studies applied to AHTR technologies, see Griveau (2007) and Fardin and Koenig (2006).

It is important to note that for all considered operating modes, the liquid salt will always be single phase. Efforts by ANL (2004, 2005) and the NRC (2008) have performed key PIRTS focusing primarily on the response of the Reactor Cavity Cooling System (RCCS) for both the GT-MHR and PBMR and the overall NGNP project respectively. These efforts provide a nice foundation for the PB-AHTR as there are several shared characteristics (single-phase working fluid, same reactor transient code validation and verification i.e. RELAP, etc...) and will be referenced where appropriate. An initial attempt at ranking key phenomena was made prior to comparing results from the respective PIRT studies in order to reduce any outside bias. An overview for the complete procedure for generating a PIRT within the CSAU framework is discussed in a wide range of publications however a simplified version of the process has been adapted for performing PIRT solely (ANL, 2005).

Table 7 PIRT Generation Procedure (ANL, 2005)

Steps	Description
Step 1	Selection of Nucleus Set of Events and Primary Safety Criteria
Step 2	Identification of Associated Components
Step 3	Identification of Major Processes and Phenomena
3.1	Identification of Accident Scenario and Phases
3.2	Identification of Major Phenomena by Components
Step 4	Ranking by PIRT Panel
Step 5	Evaluation of Knowledge Level Ranks

3.1.2 Selection of Nucleus Set of Event and Primary Safety Criteria

A list of transients considered in the Fort St. Vrain Final Safety Analysis Report (FSAR) is reproduced below and all relevant transients (transition from helium to liquid salt) have been considered in the process to determine a nucleus set of events.

Table 8 Transients considered in Fort St. Vrain FSAR

1. *Anticipated operational occurrences:*
 - a. *Main loop transient with forced core cooling*
 - b. *Loss of main and shutdown cooling loops*
 - c. *Accidental withdrawal of a group of control rods followed by reactor shutdown*
 - d. *Small break LOCA (~1 in² area break).*

2. *Design basis accidents (assuming that only “safety-related” systems can be used for recovery):*
 - a. *Loss of heat transport system and shutdown cooling system (similar to scenario 1b above)*
 - b. *Loss of heat transport system without control rod trip*
 - c. *Accidental withdrawal of a group of control rods followed by reactor shutdown*
 - d. *Unintentional control rod withdrawal together with failure of heat transport systems and shutdown cooling system*
 - e. *Earthquake-initiated trip of heat transport system*
 - f. *LOCA event in conjunction with water ingress from failed shutdown cooling system*
 - g. *Large break LOCA*
 - h. *Small break LOCA*

In addition to reviewing LBE’s for HTGR’s, other transients unique to the PB-AHTR such as a loss of heat sink event without being able to shutdown the circulator. Since the PB-AHTR runs at a low operating pressure compared to gas reactors and several other reactor concepts, the role of a traditional LOCA is a much lower priority in terms of challenging transients. The PB-AHTR is expected to operate in a wide range of regimes inside the entire design basis envelope. In order to better understand how the operating regime affects reactivity control, a description of the primary system response and key affected SSC’s is provided below by transient type. An emphasis is placed on heat removal in the primary loop as the integral system response will set the range of postulated boundary conditions of the shutdown rod system.

3.1.2.1 Steady-state Operation and Anticipate Operational Occurrences

During steady-state operation, the PB-AHTR operating parameters have been well documented (Table 4). Under power operation and normal shutdown modes, the normal heat removal path is through the IHX’s to the intermediate loop. Both the primary and the intermediate loop are configured so they can operate in either forced or natural circulation. Under power operation the intermediate loop reject heats to the power conversion system (PCS) and then to the primary heat

sink. Under shutdown conditions the intermediate loop can reject heat to the PCS when helium is circulated by motoring the generators, but the normal heat rejection path is by natural circulation heat transfer to the Shutdown Cooling System (SCS) heat exchanger. The SCS is a water-cooled heat exchanger located in the intermediate loop, which has a fluidic diode and is configured to operate in a similar manner as the DHX in the primary loop.

3.1.2.2 Response during Design Basis Events

Under DBA's heat removal occurs to the Direct Reactor Auxiliary Cooling System (DRACS), which consists of 8 DRACS heat exchangers (DHX) that reject heat by natural circulation to heat rejection heat exchangers (HRX) that are cooled by either external ambient air or water (the current baseline is ambient air). The HRX may have dampers on the inlet air flow (or valves on the inlet water flow) to reduce heat loss during normal operation. Only a fraction of the DRACS loops are required to operation to remove decay heat (nominally sized to remove 1% of full power, thus matching decay heat generation at 24 hours). The actual number of DRACS loops that must operate will be determined by reliability analysis.

3.1.2.3 Response during Beyond Design Basis Events

The capability to reject heat from the reactor vessel through the reactor cavity insulation system to the reactor cavity cooling system, or to "ground" (the building structure around the reactor vessel) will be studied under conditions where the guard vessel is faulted and the reactor cavity fills with buffer salt. This heat rejection method has not yet been studied in detail and will ultimately need to be determined however does not affect this work.

The nucleus set of events considered for the PIRT study will ultimately be the set of LBE's (see Section 3.2.4). As discussed, the LBE's are developed after an exhaustive PRA effort used to assess all potential failure modes. For the purpose of this work, the nucleus set of events are broadly classified as AOO's, DBE's, and BDBE's.

3.1.3 Identification of Associated Components

Phenomena of importance are specific to each system and component for a given nucleus set of events thus making it necessary to identify associated systems and their components for use in identifying and ranking the phenomena (ANL, 2005). A list of systems and associated components for the PB-AHTR are compiled below (Table 9).

Table 9 Identification of systems and components for the PB-AHTR

Systems	Components
Reactor Vessel	Inlet Plenum
	Core Components and Reflector
	DHX
	Outlet Plenum and Components
Reactor Primary Loop	Hot/Cold Leg
	Primary Pumps
DRACS Loop	Riser Sections
	Chimney Sections
Intermediate Heat Exchanger	Primary Side
	Secondary Side
Power Conversion System (indirect cycle)	Turbines (3)
	Recuperator
	Precoolers (3)
	LP Compressors (3)
	Intercoolers (3)
	HP Compressors (3)

Since the focus of this work is on the response of the shutdown rod system, an emphasis on the reactor primary loop system, in particular the core region is made. It has been established that the localized flow conditions affecting the shutdown rod system are governed by the overall system response which would require a PIRT study encompassing all systems and components. An initial effort to do exactly this (Fardin and Koenig, 2006) was performed on the AHTR-MI (an earlier generation of the PB-AHTR with several common design features). With the scope of the PIRT study being limited to the core region and shutdown rod channel response, it is

acknowledged that there may be missed scenarios of interest that could affect shutdown rod performance.

3.1.4 Identification of Major Processes and Phenomena

This step consists of two sub-steps: 1) identification of accident scenario and phases and 2) identification of major phenomena by components. Time constants for the various phases where they can be assessed.

3.1.4.1 Identification of Accident Scenario and Phases

- Safe Shutdown following IHX Tube Rupture

For this transient, a tube rupture due to excessive wear (i.e. fretting induced, foreign-object, corrosion, etc...) in the IHX occurs triggering a signal in the primary loop level sensor and/or radiation detection on the intermediate loop initiating a scram and run-back of the primary pumps to equalize pressure across the IHX. When the primary pumps are operating, the primary salt is at higher pressure than the intermediate salt. When the primary pumps are stopped, the intermediate salt is at higher pressure. For this transient, the control rod system does not function but the active mechanism for driving the shutdown rod system does perform as expected. This is not a very challenging transient for the PB-AHTR but serves as a good baseline for phenomena expected under normal AOOs.

Relevant phases and time scales – Safe Shutdown following IHX Tube Rupture

The first phase consists of the time period between initiation of the tube rupture and the point at which the shutdown rod active system is initiated. This actual time period is going to be the sum of the amount of time for the operations system to register a change in the primary loop (i.e. pressure at IHX exit) and the amount of time it takes to scram the reactor. According to Bartlett (1998), a conservative value of approximately 380 seconds can be assumed for an average steam generator tube rupture scram event in an LWR system. It should be noted that the loss of flibe to the secondary system will not present a safety risk but rather potentially a significant financial one. It is expected that the reactor scram for the PB-AHTR will be designed with modern diagnostic equipment to drastically reduce the amount of time it would take to shut down the reactor following this event.

Phase	Phase ID	Event Scenario and Major Processes
1	Coast down	<ul style="list-style-type: none"> • RPS detects IHX leak • Pump tripped and flow coast down starts • Active rod insertion occurs and fuel temperature decreases

LOFC Transient Without Scram

Under a LOFC transient without scram the primary pumps trip but the active shutdown drive elements do not function. RELAP5-3D simulations indicate that upon loss of forced circulation, hot coolant from the core outlet plenum flows into the top of the shutdown rod channels, while the cold fluid in the channels flows downward and out of the channel over a period of several seconds. Buoyancy forces then drive the insertion of the shutdown elements. Initial calculations indicate that this insertion occurs relatively rapidly, and thus limits the peak coolant outlet temperature and greatly delays subsequent re-criticality (Reference, 2008).

Relevant phases and time scales – LOFC Transient without Scram

In the first phase of the transient, the pumps have tripped and the primary loop is in full coast down mode. With the active reactivity control system not being initiated, the temperature in the fuel begins to rise. As mentioned above, the period until the flow switches direction and buoyancy-driven heat removal through the DRACs is several seconds as the primary pumps coast down.

The second phase of the transient represents the period of time from when the flow reverses to the time when the safety rod reaches full insertion. Since the coolant flow is now acting in the same direction as the gravity forces acting on the rod, the rod is expected to insert rapidly and stop the reaction.

Table 10 Phases for LOFC Transient without Scram

Phase	Phase ID	Event Scenario and Major Processes
1	Coast down	<ul style="list-style-type: none">• Pump tripped and flow coast down starts• Active rod insertion does not occur and fuel temperature increases• Higher pressure drop in DHX heavily retards flow
2	Buoyancy-driven	<ul style="list-style-type: none">• Pressure drop in DHX has completely reversed flow and drives coolant down core• Rapid insertion of rod driven by flow reversal• Core reaches a safe shutdown state

LOHS Transient without Scram

An important challenge for the PB-AHTR is the LOHS transient without scram, where the IHX heat removal is interrupted but the primary pumps continue to operate. This is also a severe transient for a modular helium reactor (MHR), since if forced circulation of the primary coolant continues after loss of heat removal, without scram the shutdown of the reactor on negative fuel

temperature feedback drives the circulated coolant to very high temperatures. The PB-ATHR reaches lower temperatures because it has negative coolant temperature feedback in addition to negative fuel temperature feedback. The goal in the design of the buoyant shutdown rod system is to further reduce this peak temperature under a LOHS transient without scram.

Under LOHS without scram, the coolant temperature exiting the IHX begins to rise rapidly to equal the temperature entering the IHX. After a short delay time for coolant transport, the temperature of the purge flow entering the shutdown channels begins to rise. Because this warmer coolant has lower density than the coolant in the shutdown channel, and because it is injected as a jet with relatively high velocity, the coolant mixes with relatively high effectiveness in the channel volume below the shutdown element. To first order, the rate of change in temperature in the volume below the shutdown element can then be predicted by assuming that this volume is well mixed. Preliminary calculations indicate that heat transfer to the channel walls plays a small role, with its maximum effect on the coolant temperature being below 2°C.

Because the one or more of the primary pumps do not trip under a LOHS transient without scram, the purge flow continues causing a net upward flow in the shutdown channels with velocity U_{co} . Therefore the vertically-averaged temperature of the coolant flowing around the shutdown control element must rise sufficiently so that the terminal drop velocity exceeds U_{co} , before the element will begin to drop. This makes it important to design the shutdown element to maximize its terminal drop velocity, while also maximizing its reactivity worth (Reference, 2008).

Relevant time scales – LOHS

As in the LOFC transient, the LOHS transient without scram must be broken up into a series of temporal phases. The first phase represents the period of time where the flibe exiting the IHX equals the temperature at the inlet with the pump at full operation. The actual period of time depends on how the ability to remove heat to the heat sink is compromised. For the purpose of this work, it is assumed that the heat sink is interrupted instantaneously and the period of time until the temperature at the inlet and the outlet are equal equals the volume of one of the four primary loops minus the core volume (rest of loop = rol) divided by the coolant velocity.

$$\tau_{LOHS,1} = \frac{V_{rol}}{Q_{coolant}} = \frac{30.8m^3}{1.85m^3/s} = 16.65s$$

After the IHX temperatures equalize, the primary coolant rises due to the inability to remove heat to an ultimate heat sink. The second phase represents this period and ends at the time that the negative coolant feedback starts. According to current RELAP LOHS analyses, this period of time is approximated to be 40 seconds.

$$\tau_{LOHS,2} = 40s$$

The third phase represents the period of time between the time at which negative coolant feedback sets in and when the shutdown rod begins to drop. In order to determine this period of time, RELAP simulations must again be used to determine the time at which the channel temperature reaches 615°C. Due to the uncertainty associated with the LOHS analysis, an actual value for this time phase still needs to be determined.

The fourth and final phase is the period of time from rod drop initiation to fully inserted position ($L_{channel}$). As the coolant temperature rises in the channel, the rod will start to insert faster but will also begin to suppress the reactor flux. Due to the large primary loop length and slow coolant velocities, there is a delay in the thermal response of the channel and a comparison of key time constants is necessary (see results of PIRT study).

The actual value of the time constant for phase 4 depends on a series of more advanced calculations concerning the thermal response of the primary loop and the dynamics of the shutdown rod system. In essence, the focus of the PRISM separate effects experiment (Section 4) is to determine this time constant given a range of boundary and initial conditions. Key phenomena associated with each phase of these scenarios are discussed later in this section.

Phase	Phase ID	Event Scenario and Major Processes
1	IHX thermal relaxation	<ul style="list-style-type: none"> • Ability to remove heat to ultimate heat sink is compromised • Pump is <u>not</u> tripped • Active rod insertion does not occur • Temperature of IHX outlet climbs to inlet temperature
2	Forced convection with no reactivity feedback	<ul style="list-style-type: none"> • Coolant temperature driven up by no slowing down of reaction • No reactivity control • Mass flowrate does not change
3	Forced convection with reactivity feedback	<ul style="list-style-type: none"> • Negative coolant feedback effects start to bring down fuel temperature but still increasing • No reactivity control • Mass flowrate does not change
4	Forced convection with reactivity feedback and shutdown rod insertion	<ul style="list-style-type: none"> • Temperature of shutdown rod channel reaches critical point and rod begins to insert into channel • Negative coolant feedback effects • Mass flowrate does not change • Core reaches a safe shutdown state

3.1.4.2 Identification of Major Phenomena by Components and Ranking by PIRT Panel

Integral effects phenomena refer to processes that consist of more than one basic heat transfer or

fluid phenomenon as opposed to separate effects (Levy, 1999). The combined behavior of these phenomena is of particular interest to the engineer modeling the system and creates the major goals and requirements in design of a scaled model test facility. Key phenomena are identified in this section by affected component and evaluated by the aforementioned accident temporal phases. Since the dynamic response of the shutdown rod system is driven by the thermal response of the flibe in the shut down rod channel, all relevant phenomena related to PB-AHTR core, plenum, and primary system thermal-hydraulics and neutronic response must be considered. For heat transfer in the shutdown rod channel, the flibe will be in forced, mixed, or natural convection heat transfer modes. In terms of flow regimes, the flibe in the channel will either be laminar, transition to turbulent or turbulent flow. For each of these regimes, a corresponding friction factor correlation exists that determines the pressure drop across the core (ANL, 2004).

Table 11 Possible flow regimes and corresponding heat transfer modes (ANL, 2004)

Forced convection Turbulent flow	Forced convection Transition to turbulent flow	Forced convection Turbulent flow
Mixed convection Turbulent flow	Mixed convection Transition to turbulent flow	Mixed convection Turbulent flow
Natural convection Turbulent flow	Natural convection Transition to turbulent flow	Natural convection Turbulent flow

Flow is introduced into the shutdown rod channel in the form of a turbulent jet from a nozzle located just above the hydrodynamic arresting channel. In a postulated accident where the primary coolant is rising in temperature, the injected jet becomes buoyant and affects the thermal-hydraulic response of the channel. An analysis of the phenomena associated with the entrance jet and thermal mixing in the channel is provided in Appendix B. A list of key phenomena are presented and ranked in the following tables by component. As discussed, previous PIRT efforts concerning high temperature reactors has provided a wide range of potential phenomena based on several expert panels. While the results of the table ranking process were not examined prior to assembling the following tables, the relevant phenomena for similar components were compared to make sure nothing was mixed. It should be noted that H, M, and L refer to High, Medium, and Low for phenomena ranking.

Inlet/Outlet Plenum

Table 12 PIRT table for inlet plenum

Phenomena	Safe Shutdown		LOFC		LOHS			
	1	2	1	2	1	2	3	4
Phase								
Flow distribution								
Heat transfer (forced convection)								
Heat transfer (mixed convection)								

Heat transfer (natural convection)								
Thermal mixing and stratification								
Jet Discharging Into a Plenum								
Pressure drop (natural convection)								
Pressure drop (mixed convection)								
Pebble distribution?								
Conduction								

Core (excluding shutdown rod channel)

Table 13 PIRT table for core region (without shutdown rod channel)

Phenomena	Safe Shutdown		LOFC		LOHS			
	1	2	1	2	1	2	3	4
Flow distribution								
Heat transfer (forced convection)								
Heat transfer (mixed convection)								
Heat transfer (natural convection)								
Thermal mixing and stratification								
Pressure drop (natural convection)								
Pressure drop (mixed convection)								
Pebble distribution								
Initial stored energy								
Power distribution								
Decay heat								
Radiant Heat Transfer								
Spatially Non-Uniform Heat Flow in Thick-Walled Structure at Steady State								
Temperature Profile in Thick-Walled Structure During Transient								
Thermal Striping								
Abrupt Flow Change								
Multi-Fluid Coolant								

Shutdown rod system (including shutdown rod channel)

Table 14 PIRT table for core region (without shutdown rod channel)

Phenomena Phase	Safe Shutdown		LOFC		LOHS			
	1	2	1	2	1	2	3	4
Flow distribution (buoyant jet insertion)								
Thermal mixing and stratification (buoyant jet effects)								
Pressure drop (natural convection)								
Pressure drop (mixed convection)								
Hydrodynamic forces acting on rod (i.e. cross flow “pinning”, jet switching, etc...)								
Radiant Heat Transfer								
Spatially Non-Uniform Heat Flow in PCA at Steady State								
Temperature Profile in PCA During Transient								
Thermal Striping								
Abrupt Flow Change								
Multi-Fluid Coolant (i.e. buffer salt intrusion)								

3.1.5 Evaluation of Knowledge Level Ranks

With a lack of experimental data for comparable reactor systems, the level of knowledge associated with molten salt reactors is pretty limited. Operational data is available but overall the knowledge level associated with liquid salt reactors is significantly lower than HTGRs. However, key components of the PB-AHTR such as the graphite PCAs, TRISO fuel, and DRACS system, for example, are shared technologies and have been studied extensively. Therefore, key phenomena associated with most of the components in the PB-AHTR have been studied however the integral response of these components within the system has not.

4 Passive Rod Insertion Shutdown Model (PRISM) Experiment

In order to demonstrate the viability of the passively-driven shutdown rod concept, a proof-of-principle experiment is necessary to validate computer simulations. Scaled test facilities have played a critical role in LWR reactor licensing (see Section 2.2 for further discussion) and are used extensively in a variety of different industries. A scaled model of the PB-AHTR shutdown rod system was built in the UC Berkeley Nuclear Engineering Thermal-hydraulics laboratory using sugar water as stimulant fluid. A description of the experimental setup and work performed is discussed in this section.

4.1 Sizing of the PRISM Experiment

Properly scaled experiments maintain geometric, kinematic, and dynamic similarity between the model and the prototype (throughout this section, the subscripts p and m refer to prototype and model respectively). Demonstration of physically similar phenomena is essential to success for modeling. Physical phenomena are considered similar if they differ only in numerical values of the dimensional governing parameters; the values of the corresponding dimensionless parameters Π_1, \dots, Π_m (Barenblatt, 1996). These similarity parameters are discussed further below.

4.1.1 Geometric similarity

Geometric similarity involves the length parameter and is usually desirable for modeling efforts. The scales for length and mass flux for a water model of a flibe prototype at 700°C can be calculated by preserving the Froude and Reynolds numbers, giving (Bardet, 2007).

$$Fr = \frac{U}{\sqrt{gh}} = \frac{q}{\sqrt{L}} \cdot \frac{1}{\rho} \quad , \quad Re = \frac{UL}{\nu} = qL \cdot \frac{1}{\mu}$$

$$\left(\frac{L_m}{L_p} \right)^{3/2} = (L_r)^{3/2} = \frac{\nu_m}{\nu_p} \quad \Rightarrow \quad L_r = 0.463$$

Additionally, all angles in the system must be preserved from the prototype to model geometry. The shutdown rod channel geometry is cylindrical with prototype and model dimensions tabulated in Table 15.

Table 15 Prototype and model channel dimensions

	PB-AHTR 900 MWth	PB-AHTR Pilot Plant	PCRS
Working fluid	Flibe	Flibe	Sugar water
Active height	6.2 m	6.2 m	2.87 m
Channel diameter	19.8 cm	19.8 cm	9.16 cm
Flow area	0.0308 m ²	0.0308 m ²	6.6E-3 m ²
Diameter of jet orifice	6.26 cm	6.26 cm	2.90 cm
Jet-to-channel density ratio	0.974	0.974	0.974

In addition to the shutdown rod channel, the shutdown rod must also be scaled down to the appropriate size in order to maintain Froude and Reynolds numbers. Due to the complex geometry of the shutdown rod and the fact the PCRS experiment is proof-of-principle, a simple geometry was selected for the shutdown rod model. This change in geometry will have a significant effect on the parasitic drag forces acting on the shutdown rod. Maintaining dynamic similarity between the model and prototype is discussed in Section 4.1.3 while results for the optimized design are tabulated in Table 16.

Table 16 Prototype and model shutdown rod dimensions

	PB-AHTR 900 MWth	PB-AHTR Pilot Plant	PCRS
Effective rod length	3.5 m	3.5 m	1.621 m
Effective rod diameter	0.13 m	0.13 m	0.045 m
Shape drag coefficient	TBD	TBD	~1.9
Density of rod material	1.980 g/cm ³	1.980 g/cm ³	1.022 g/cm ³

4.1.2 Kinematic similarity

Kinematic similarity in itself implies geometric similarity and in addition that the ratio of the velocities at all corresponding points is the same. The velocity ratio, V_r , is expressed below and its value in terms of L_r is determined by dynamic considerations in the next section.

$$V_r = \frac{V_p}{V_m}$$

Using the length scale determined in Section 4.1.1, the time scale can be determined using the following relationship.

$$T_r = \frac{L_r}{V_r}$$

The above two relationships are used to determine the overall response of the PB-AHTR shutdown rod during a transient. These results are presented later in Section 4.5.

4.1.3 Dynamic similarity

Maintaining dynamic similarity between the model and the prototype means the corresponding forces must be in the same ratio. As described in Section 3.2.1, the forces acting on the rod are a combination of buoyancy and drag. The buoyancy force acting on the shutdown rod is a strong function of temperature. For the PCRS to be dynamically similar the following relationships must hold true:

$$\frac{F_{B,m}}{F_{B,p}} = \frac{F_{D,m}}{F_{D,p}}$$

Since the simplified shape of the shutdown model rod is quite different than the actual PB-AHTR shutdown rod geometry, the ratio of pressure to viscous drag will differ for both systems. Therefore, the dynamic response of the rod in the model will not be a direct representation of the PB-AHTR SRS as some distortion exists between the corresponding drag forces. Future work for the PRISM experiment includes the fabrication of a geometrically similar model shutdown rod.

4.2 PRISM Description

The water loop for the PRISM experiment was assembled using inexpensive PVC and acrylic piping. An optics table was used to mount the shutdown rod channel model and for providing overall structural support. Flow in the loop is throttled using a simple PVC ball valve where volumetric flow rate is determined using a rotameter. All couplings were off the shelf components with a preference towards rigid tubing. Due to the height of the channel, supports were built off the table and off of the ceiling to dampen flow-induced vibration and provide structural support. For regions of interest, acrylic piping was used to allow for visual inspection. PRISM was designed to be modular allowing for the replacement of entire loop sections (see end of section for discussion on future work). A schematic for the PRISM experiment is included below (Figure 0-1) and depicts the overall loop structure. A description of key equipment and measurement tools is given below.

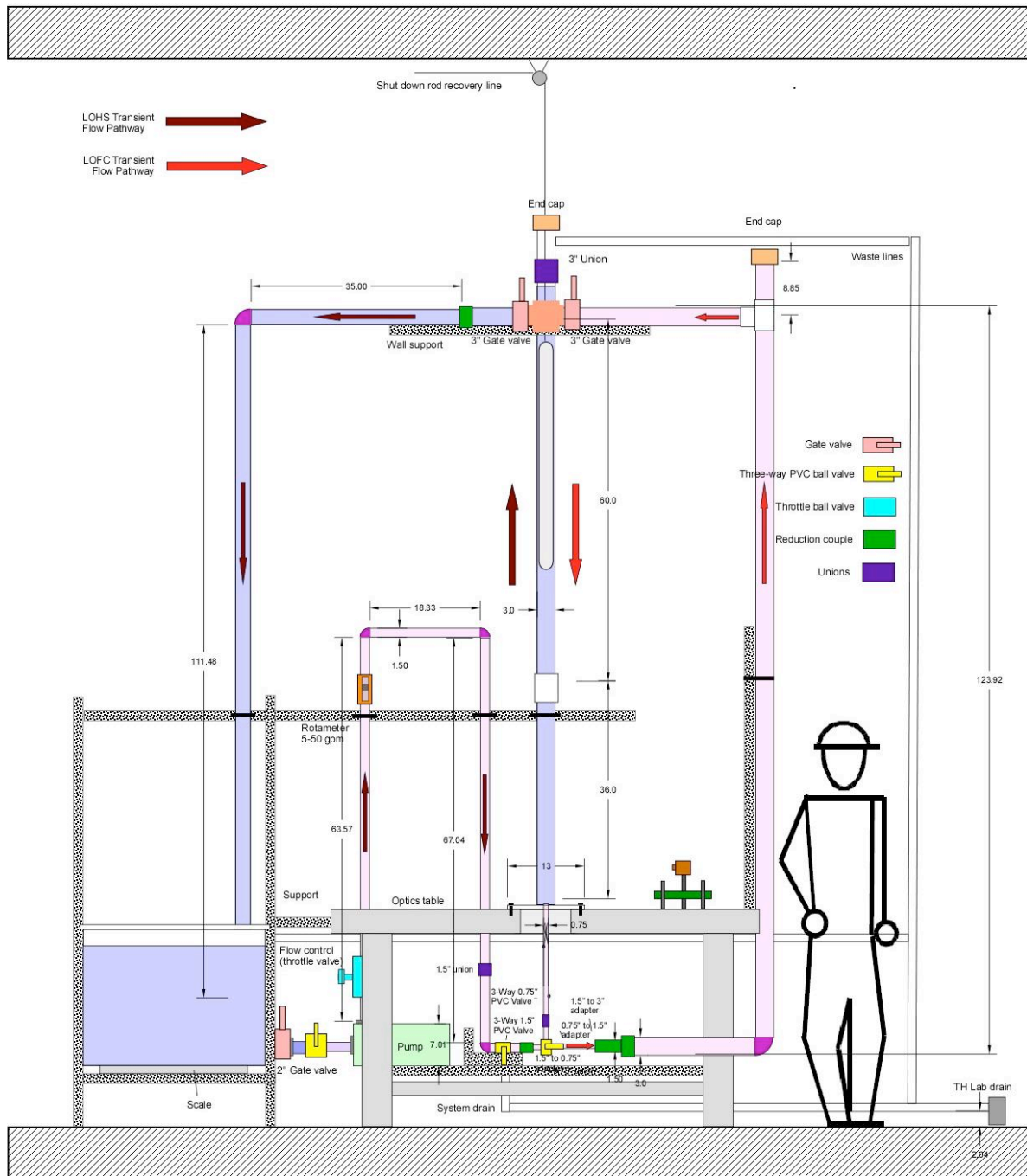


Figure 0-1 Schematic of PRISM experiment and key components

The initial shutdown rod model was fabricated using stock PVC material and piping. A streamlined shape was machined on a lathe to minimize form drag and Teflon gaskets were used in conjunction with a stainless steel threaded rod to both tighten the two caps and to also provide a means for adding and distributing mass (washers) in the rod. A picture of the shutdown rod can be found below (Figure 0-3).

Key functional equipment for the PRISM experiment besides the piping infrastructure and optics table include:

- Centrifugal Pump
 - HP
 - Power Source
 - RPM etc
- Water tanks
 - 43 gallon vertical polyethylene
 - 44 gallon vertical polyethylene
- Throttle valves
 - 1 ½” PVC ball valves
- Neodymium recovery magnet
- Shutdown rod model snubber

Key measurement equipment for the PRISM experiment include:

- Asayo ML330 weighing digital scale
 - Capacity 330 lb (150 kg)
 - Accuracy .05 lb (.02 kg)
 - Precision over 5000 divisions
 - Exceeds OIML III Standard
- Lab scale
 - Capacity 400 g
 - Accuracy +/- 0.005 g)
- Rotameter
 - 1 ½” Flowmeter 5 - 50 GPM
 - +/- 6% Accuracy
 - Stainless steel float

A picture of the final PRISM experiment setup for the initial phase is below. Unistrut and wood was used to make the loop structure and the tank housing structure. In order to access the top of the loop, a ladder was used to both recover and reposition the shutdown rod model. In the next section, a process for initially calibrating PRISM is discussed in addition to experimental uncertainties.



Figure 0-2 PRISM experiment prior to calibration runs



Figure 0-3 Pictures of the shutdown rod assembled and disassembled (yardstick provided for reference)

4.3 Experimental Results

4.3.1 Initial Calibration

In order to collect meaningful data, PRISM needs to be initially calibrated to determine overall measurement accuracy and associated experimental uncertainties. Key information such as the rod volume and exact density are difficult to measure to a required high degree of accuracy separately without appropriate lab equipment, therefore calibration of PRISM was done by understanding the density of the rod relative to the density of the sugar water in solution. Given the large amounts of experimental data available on sugar water solutions, it was decided that mass measurements would introduce the least amount of experimental error for determining the density difference of both the rod and solution as opposed to treating the weight and buoyant forces separately.

The shutdown rod is designed to be neutrally buoyant at 615°C under prototypical conditions which corresponds to a sugar water specific gravity of 1.0225. Using experimental results from Greenwood (1999), a relationship between specific gravity and sugar water concentration

(weight percent) was determined. With the shutdown rod in the PB-AHTR expected to operate under a range of buoyancy forces going from positive (steady-state) to negative (higher temperatures), the difference in buoyancy force as a function density gradient between the rod and coolant is the key variable of interest. Therefore, a solution of sugar water with a SG of 1.0225 (5.71% SW) was assembled in a calibration apparatus consisting of 4" ID acrylic tubing (see Figure 0-4). Prior to mixing the sugar, the apparatus was dried and measured using the Asayo scale. In addition, the model shutdown rod was dried and weighed using the same scale. It should be noted that the water used to calibrate the shutdown rod model was left out overnight in a separate reservoir to equilibrate with room conditions (the same technique is used for data collecting runs). Given the relatively large volume of the calibration apparatus, 6.0 kg of water are added after taring the scale including the apparatus and stirrer. In order to achieve a 5.71% SW mixture, 363.1 g of sugar was added to the solution and the weight was independently verified using the Asayo scale. Using the stirrer, the solution is mixed in order to achieve a uniform concentration. The rod is then inserted in order to determine the required mass necessary to make the rod neutrally buoyant in the solution. For the first run, washers are added to the magnet on the top of the rod to add mass. Once the required mass is determined, the rod is removed and the washers are installed inside the rod and the rod is reinserted to assess any potential volume issues the external washers may have caused. While a small amount of mass of solution will be lost during this step, the impact should be minimal as the solution is well mixed and we are only concerned about the SG of the solution.



Figure 0-4 Calibration apparatus for shutdown rod and Asayo scale

Table 17 Initial calibration data

Item	Measurement
Shutdown rod model (number of washers)	1.5 kg (44)
Washer	8 g (+/- 0.4 g)
Calibration apparatus	4.82 kg
Stirrer	245 g
Water	6.0 kg
Sugar	363.1 g

Once the density of the rod is adjusted to be neutrally buoyant at the simulated 615°C temperature, phase I of data collection begins. It should be noted that when PRISM was initially run, the shutdown rod model was being forced against the side of the channel due to the cross flow exiting the channel. A restrictor orifice was fabricated and positioned several pipe diameters below the exit channel and minimizes any forces in the horizontal direction (see Figure 0-5).

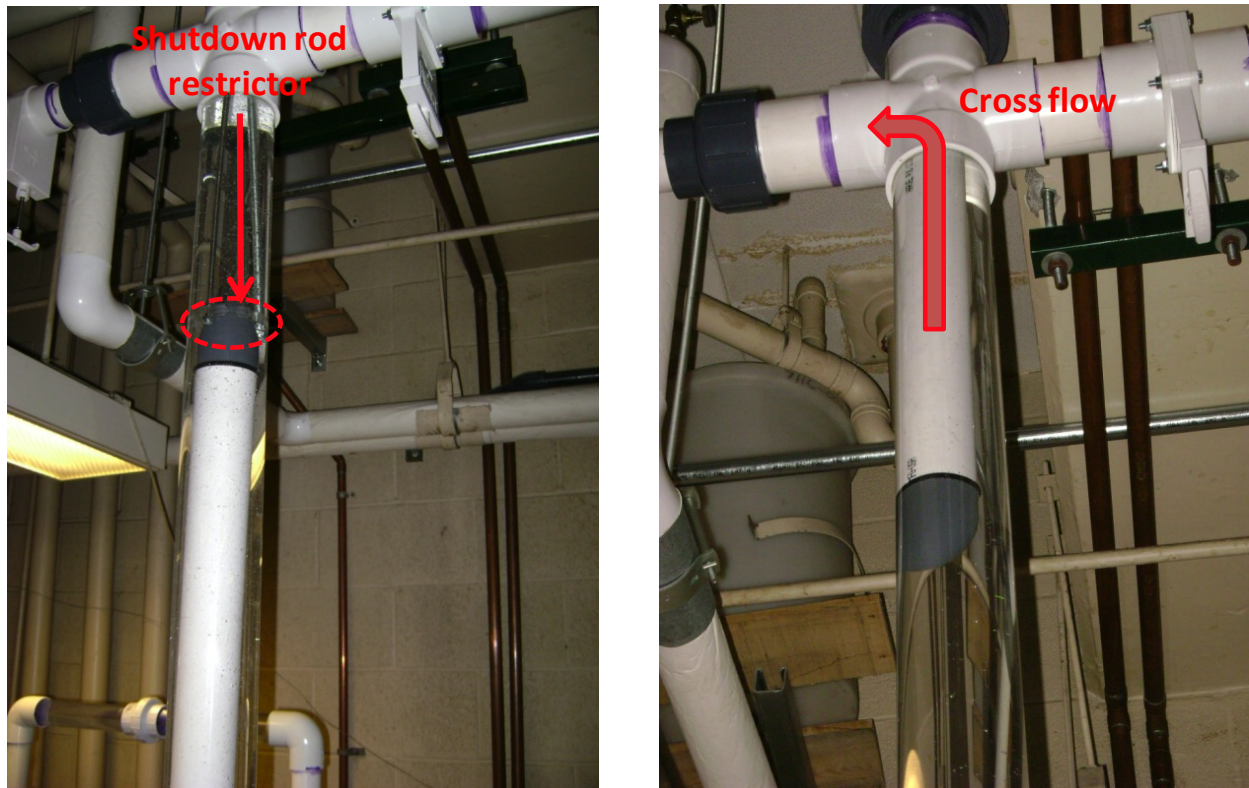


Figure 0-5 PRISM loop with and without shutdown rod restrictor in place

4.3.2 PRISM Transient Simulations

Phase I: Drag Coefficient as a Function of Reynolds Number

For Phase I of data collection for PRISM (initial calibration), the drag coefficient of the shutdown rod is determined in both stagnant and counterflow fluid conditions as a function of Reynolds number. The rod drag coefficient, C_D , will be a function of the rod Reynolds number, rod and channel diameters, and potentially the ratio of the coolant upflow speed due to bypass flow, U_C , to the rod velocity relative to the coolant flow, U_R . When dropped under static liquid conditions, the terminal velocity of the shutdown rod is reached when the buoyant forces of the rod equal the drag forces.

$$C_D = \frac{\Delta\rho V_{rod} g}{\rho_{fluid} A_{cs} U_R^2}$$

Where the numerator, which is the net buoyancy force (function of the density difference between the rod and the fluid), can be rewritten as,

$$\Delta\rho V_{rod} g = \Delta m g$$

In order to minimize excessive experimental error in measuring the density of the sugar water solution, density is varied by adding mass to the rod in the form of additional washers. By increasing the mass of the shutdown rod model and keeping the same volume and operating conditions (flowrate, fluid density, temperature etc...), the only additional source of error will be the uncertainty in the mass of the shutdown rod. The accuracy of this calculation is just then,

$$\delta\rho = \frac{\delta m}{V_{rod}} = \frac{m_w}{V_{rod}}$$

where m_w is the mass of the washer. The rod is dropped multiple times under both stagnant and counterflow conditions and the velocity is measured by hand using a stopwatch and a previously marked off region of the channel. It was decided that the time measurements would be made towards the bottom of the channel in order to measure the rod's terminal velocity. A minimum of three timed runs were performed for each density change of the rod where the averaged value is used in determining the rod drag coefficient. As expected, hand timing using a marked backdrop introduces a significant amount of experimental error especially at high rod Reynolds numbers where the rod is moving quickly and it is difficult to accurately time. In section 4.4, future work is discussed where an automated system to measure velocity is introduced. Tabulated results are presented in Appendix C and a plot of drag coefficient versus the rod Reynolds number is presented in Figure 0-6.

$$Re = \frac{\rho_{fluid} U_r D_r}{\mu_{fluid}}$$

where $D_r = 4A_r/P_r$ is the hydraulic diameter of the rod, and P_r is the wetted perimeter of the rod frontal area. For all trials, the flow was throttled until the rotameter read 13 GPM and not adjusted when rod mass was changed. All fluid properties remain constant so only the rod insertion velocity will change with increasing mass.

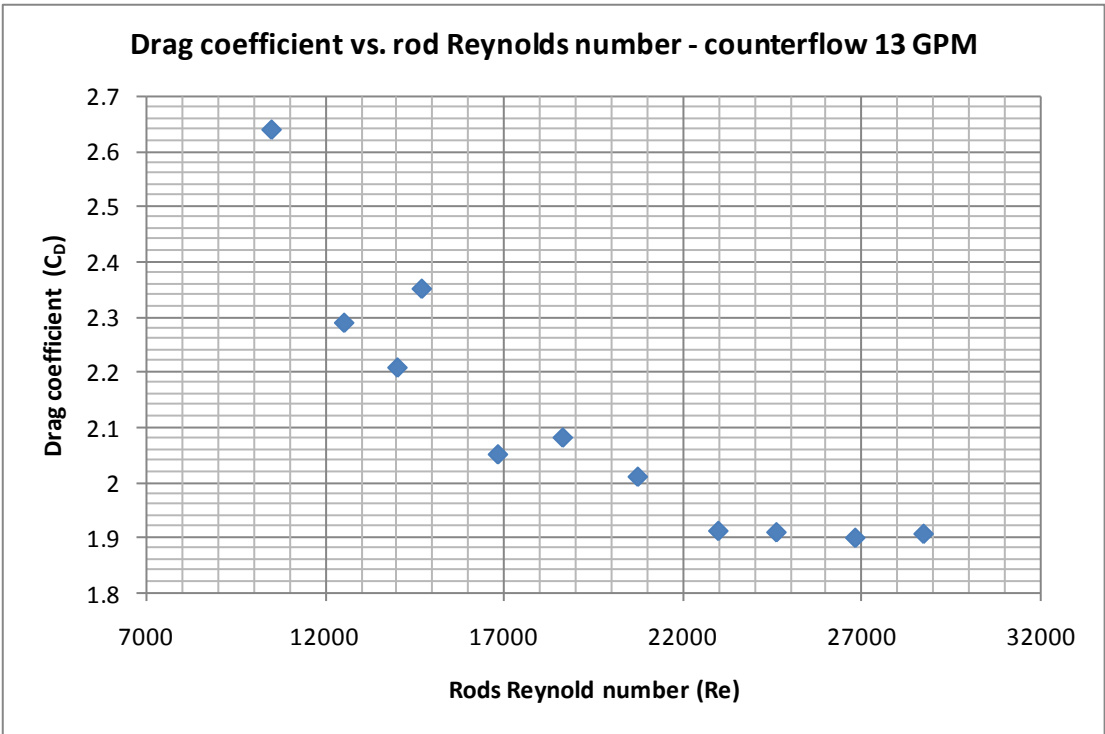
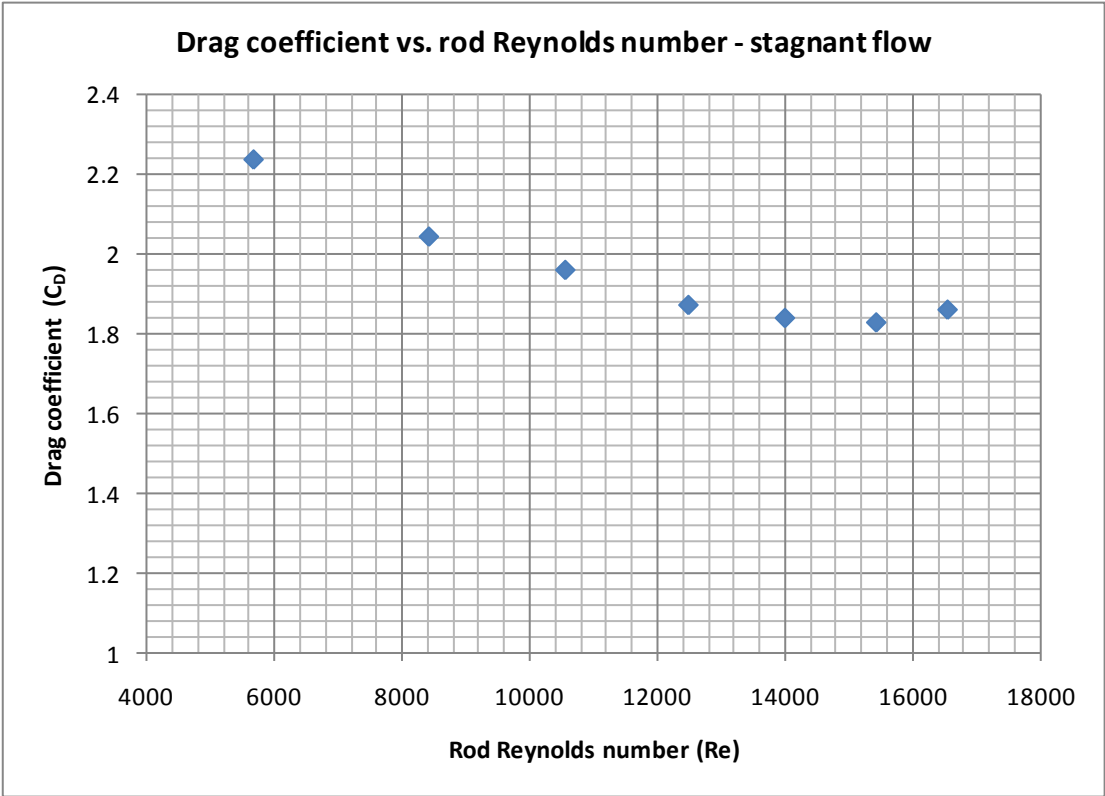


Figure 0-6 Drag coefficient vs. rod Reynolds number for both stagnant and counterflow conditions

Phase II: Response of Shutdown Rod during LOFC Transient

In the event of a LOFC transient, flow reversal in the core occurs due to the onset of natural circulation. To simulate this transient, the second loop is used (see Figure 0-2) and the LOHS loop is isolated. To do this, the gate valve restricting the LOHS simulation flow is closed and the channel is filled with steady-state equivalent sugar water density while the remainder of the loop is filled with pure water with a lower density making sure the gate valve separating the channel from the remaining loop and the three-way valve at the bottom of the channel are closed. The transient is initiated by opening both valves simultaneously and monitoring the response of the channel and rod. The density gradient should drive the sugar water down and then up into the opposite channel while the fresh water should flow across and down the shutdown rod channel forcing the rod to fall. While the onset of natural circulation through the core does not occur instantaneously, this “step-change” simulation represents the bounding response of the rod during this transient. A series of simulations will be performed in this phase with a range of density differences to study the response of the rod.

Phase III: Response of Shutdown Rod during LOHS Transient

Before experimentally simulating the LOHS transient in PRISM, a pre-predictive model must be developed to model the response of the shutdown rod. The governing equations (i.e. mass, momentum, and energy) are given in Appendix A where appropriate control volume and finite difference methods for solving this problem are discussed.

The amount of time necessary to heat up the core to 615 °C can be determined using the following relationship:

XXX

4.4 Future PRISM Work

LASER PHOTOGATE SYSTEM

GEOMETRIC SIMILAR ROD

The two most pressing modifications planned for the future include:

- Construction of a clear acrylic window surrounding the buoyant jet insertion region allowing for minimal optical distortion during ink injection visualization studies
- Construction of a clear acrylic window just downstream of the jet inlet region allowing for independent in-situ density measurements using a transverse laser

5 Methods for Assessing Passive Safety System Reliability – Case Study: SRS

Reliability engineering became a formal discipline during World War II due to unacceptable failure rates in electronic equipment that Allied troops depended on. Repair costs and maintenance oftentimes exceeded up to ten times the original cost (Dodson, 1999) and the idea of life cycle costs was subsequently developed. Reliability engineering is a discipline for applying scientific know-how to a system, structure, component or process so it will perform its intended function, without failure, for the required time duration when installed and operated correctly in a specified environment. Simply stated, reliability is just the probability that an item will perform a required function without failure under stated conditions for a stated period of time (Military Handbook, 1998). It is important to note the words “under stated conditions” which is very relevant to the proposed scenario-based approach to risk and reliability assessment.

The focus of this section is on safety systems and components in a nuclear power plant that fall either into an active or passive category. According to IAEA (1991), passive components and systems are defined as follows,

Passive Component: a component which does not need external input to operate.

Passive System: either a system which is composed entirely of passive components and structures or a system which uses active components in a very limited way to initiate subsequent passive operation

Passive systems are subsequently categorized by type with some examples (IAEA, 1991),

- Type A: physical barriers and static structures,
 - i.e. Reactor Cavity Cooling System (RCCS) chimney structure, fluidic diode, heat exchanger tubes
- Type B: moving working fluids,
 - i.e. Buoyantly-driven air flow in RCCS, gravity driven cooling system
- Type C: moving mechanical parts,
 - i.e. Check valves, filtered venting systems, buoyant shutdown rod
- Type D: external signals and stored energy (passive execution/active actuation)
 - i.e. Electromagnetic control rod initiation

On the other hand, active systems require some element of electrical or mechanical signal to initiate and/or operate. Traditionally, LWR safety systems have been extensively active with thousands of years of reactor experience now providing excellent component reliability data for predicting system and component performance. Likewise extensive progress has occurred in assessing the reliability of “Type A” passive systems due to advances in structural mechanics

and material degradation studies which has led to development of extensive material codes and standards for the design of “Type A” passive systems. While the PB-AHTR presents a set of challenges to this class of passive systems, the focus of the research study reported here is on Type B and C passive systems with an emphasis on the reliability of the buoyantly-activated PB-AHTR shutdown rod system. As discussed in Section 3.2.4, the reliability of these types of safety systems plays a very important role in performing PRA. It has become commonplace to assume that the shift towards passive system improves reliability however it has been shown by Pagani (2005) that active systems, in some cases, can be designed to be more reliable than passive systems when accounting for functional failure. In Pagani’s particular work, the case study considered the reliability assessment of forced and natural cooling options for the reactor cavity in a GFR. The role of functional failure and associate uncertainties is discussed later in this section.

5.1 Failure Modes for the Safety Shutdown Rod System

According to Burgazzi (2004), the reliability of a passive system should generally be seen from two main aspects:

- Systems/components reliability (e.g., piping, valves, core support structures);
- Physical phenomena reliability (e.g., natural circulation stability, surface emissivity predictability)

System and component reliability methods for passive systems should be commensurate with the determination of the reliability of equivalent active systems. In the case of the PB-AHTR SRS, the role of “component reliability” (i.e. maintaining shutdown rod channel geometry) is of particular importance. However the overall system response of the PB-AHTR during beyond design basis operating conditions has a large impact on physical phenomena reliability. Additionally, because the SRS also has an active insertion mechanism, the overall reliability of the SRS also includes the reliability of active and structural modes. A high level fault tree diagram for the SRS has been developed below depicting all general failure mode types:

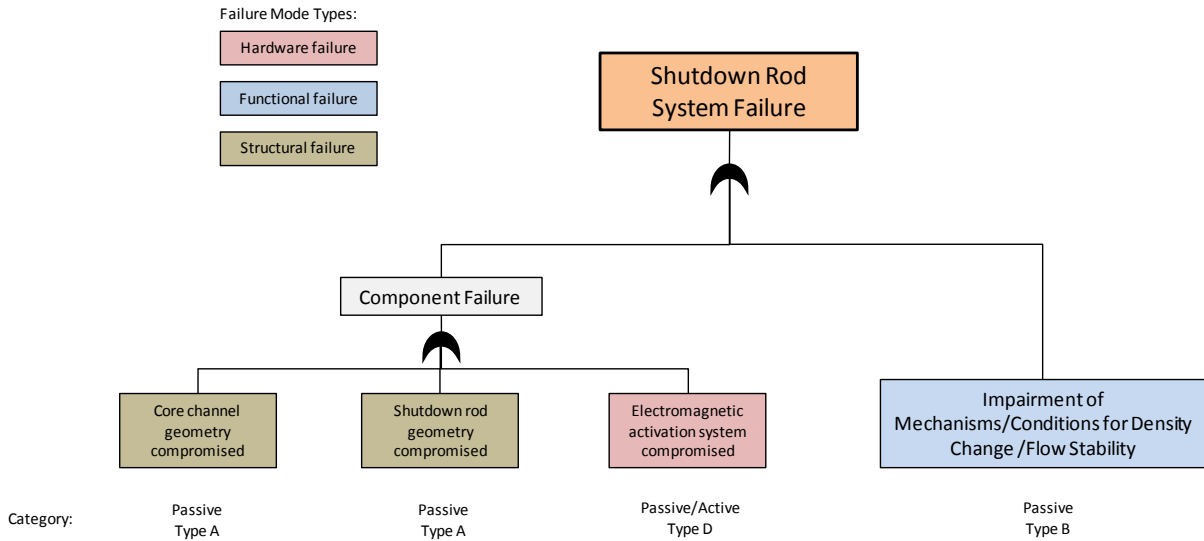


Figure 0-1 High level failure mode tree diagram

The physical phenomena reliability component is concerned with the way the natural physical phenomena evolves over the course of a transient and is the focus of functional failure modes. According to Burgazzi (2004), functional failure occurs whenever the applied “load” exceeds the component “capacity” when operating within a reliability physics framework. Using Burgazzi’s work as a basis, the overall probability of failure of the SRS will just be:

$$Pe_t = 1.0 - ((1.0 - Pe_1) \cdot (1.0 - Pe_2) \cdot \dots \cdot (1.0 - Pe_n))$$

Where Pe_t is the overall SRS probability of failure, and Pe_1 through Pe_n are the individual probabilities of failure pertaining to each of the three failure modes, assuming mutually independent events.

The failure mode relative to each single basic event is given by,

$$Pe_i = \int p_i(x) dx \quad x < x_0$$

Where $p_i(x)$ is the probability distribution function of the parameter x and x_0 is a threshold value according to the failure criterion.

Once all the failure modes have been identified, a bottom-up approach called Failure, Modes, Effects and Analysis (FMEA) is used to further investigate each mode using deductive methods. The uncertainties associated with each probability distribution assignment vary with failure mode and are discussed further in Section 5.2. For example, the uncertainties associated with functional reliability are based on failure of the physical principle (i.e. a sufficient drop in primary coolant density) and sources of these uncertainties have been identified during the PIRT process in Section 4. The reliability of the system is determined in Section 5.3 directly by assigning probabilistic distributions to the parameters for each failure mode. Due to the novel

nature of the SRS design, there is no existing operational data and the only test data has come from work performed here with the PRISM experiment. In Section 6, discussion can be found on how reliability data can be collected using an augmented experimental program.

5.1.1 Structural Failure Modes

Structural failure modes refer to situations where the geometries of the shutdown rod channels and shutdown rods are compromised. The level to which the geometry is compromised (i.e. minor wear affecting shutdown rod vs. substantial displacement of PCA blocks) has a significant effect on the overall risk that failure mode poses. In order to initially determine all the individual structure failure modes, a more detailed structural fault tree diagram was created (Figure 0-2).

External events that may affect the core geometry include hazards such as large magnitude earthquakes or large aircraft crashes. While the PB-AHTR is seismically base-isolated, a finite probability exists that an earthquake could cause sufficient damage to the core geometry. This particular failure mode must be further studied and associated risks must be assessed.

Internal events that may affect the geometry of the shutdown rod channel include PCA failure, foreign object event, or overall channel degradation. Typically these types of failure modes occur due to poor manufacturing and/or material degradation due to irradiation and/or thermal, irradiation and residual material stresses. Inspection techniques are used to monitor for potential degradation modes and to reduce overall probability of failure. The role of inspections is discussed in greater detail later.